Limited effects of xylem anatomy on embolism resistance in cycad leaves

Guo-Feng Jiang[1,*], Bo-Tao Qin[1], Yu-Kun Pang[1], Lan-Li Qin[1,2], Luciano Pereira[3], Adam B. Roddy[4]

[1]Guangxi Key Laboratory of Forest Ecology and Conservation, Guangxi Colleges and Universities Key Laboratory for Cultivation and Utilization of Subtropical Forest Plantation, and State Key Laboratory for Conservation and Utilization of Subtropical Agro-Bioresources, College of Forestry, Guangxi University, Daxuedonglu 100, Nanning, Guangxi 530004, PR China

[2]College of Chemistry and Bioengineering, Hechi University, Yizhou, Guangxi 546300, PR China

[3]Institute of Botany, Ulm University, Albert-Einstein-Allee 11, 89081 Ulm, Germany

[4]Institute of Environment, Department of Biological Sciences, Florida International University, Miami FL 33199 USA

*** Corresponding author:** Guo-Feng Jiang (gfjiang@gxu.edu.cn)

ORCID

GFJ: https://orcid.org/0000-0002-3221-8608

ABR: https://orcid.org/0000-0002-4423-8729

Word counts:

Total word count (excluding summary, references and legends):	6413	No. of figures:	8 (all in colour)
Summary:	192	No. of Tables:	6
Introduction:	1564	No. of Supporting Information files:	1
Materials and Methods:	2149		
Results:	912		
Discussion:	1788		

Summary

- Drought-induced xylem embolism is a primary cause of plant mortality. Although ~70% of cycads are threatened by extinction and extant cycads diversified during a period of increasing aridification, the vulnerability of cycads to embolism spread has been overlooked.

- We quantified the vulnerability to drought-induced embolism, pressure-volume curves, *in situ* water potentials, and a suite of xylem anatomical traits of leaf pinnae and rachises for 20 cycad species. We tested whether anatomical traits were linked to hydraulic safety in cycads.

- Compared to other major vascular plant clades, cycads exhibited similar embolism resistance to angiosperms and pteridophytes but were more vulnerable to embolism than non-cycad gymnosperms. All 20 cycads had both tracheids and vessels, the proportions of which were unrelated to embolism resistance. Only vessel pit membrane fraction was positively correlated to embolism resistance, contrary to angiosperms. Water potential at turgor loss was significantly correlated to embolism resistance among cycads.

- Our results show that cycads exhibit low resistance to xylem embolism and that xylem anatomical traits–particularly vessels–may influence embolism resistance together with tracheids. This study highlights the importance of understanding the mechanisms of drought resistance in evolutionarily unique and threatened lineages like the cycads.

Keywords: Xylem cavitation, hydraulics, drought induced embolism resistance, tracheid bordered pits, PV curve, cycads, xylem anatomy, water stress

Introduction

Cycads have long been considered a relict of a once more diverse and globally distributed group (Mamay, 1969; Brenner *et al.*, 2003). Cycads likely originated on the Laurasian landmass during the Carboniferous and expanded on Gondwana during the Jurassic (Coiro *et al.*, 2023). Despite exhibiting little gross morphological change over the last 330 million years, molecular evidence suggests that modern cycads recently and rapidly diversified during the Neogene, a period marked by increasing aridity (Nagalingum *et al.*, 2011; Condamine *et al.*, 2015; Coiro *et al.*, 2023). Current cycad diversity encompasses 367 extant species in ten genera belonging to two families (Cycadaceae and Zamiaceae) (Calonje *et al.*, 2022), of which 68% are threatened with extinction (IUCN, 2022). Extant cycads occur across a wide range of habitats, including both mesic and xeric habitats, forest understories, and open habitats (Norstog & Nicholls, 1997; Hill *et al.*, 2004; Zhang *et al.*, 2015). This

diversity in habitat and their diversification during a period of global aridification suggests that hydraulic physiology and drought tolerance may have been important in shaping cycad ecological niches. Given the current threats of climate change and human disturbance, there exists increasing urgency to understand and conserve cycads.

Globally, forests are threatened by rising temperatures and droughts, which push plants past their physiological thresholds, leading to hydraulic failure (Choat *et al.*, 2012; Adams *et al.*, 2017; Brodribb *et al.*, 2020; Tavares *et al.*, 2023). As water availability declines, leaves lose turgor pressure and air embolisms can spread through the xylem (Tyree & Sperry, 1989; Brodersen *et al.*, 2019). Resistance to embolism formation and spread, therefore, has been an important component of xylem evolution and diversification into ever-drier habitats (Pittermann *et al.*, 2010; Pittermann *et al.*, 2012; Larter *et al.*, 2017; Skelton *et al.*, 2021; Bouda *et al.*, 2022). Embolism resistance is typically quantified from vulnerability curves (VCs) that depict the relationship between water potential and the percent decline in hydraulic capacity, with critical thresholds considered to be key indicators of drought tolerance (e.g. P_{12}, P_{50}, P_{88} that represent water potentials at 12%, 50%, 88% declines in hydraulic capacity or the percentage of air discharged from the xylem). In addition to exhibiting differences in the vulnerability to embolism spread, plants can also exhibit differences in how closely they operate to these critical embolism thresholds, termed hydraulic safety margins (HSMs) (Choat *et al.*, 2018; Brodribb *et al.*, 2020; Tavares *et al.*, 2023). HSMs are calculated as the difference between critical water potentials, such as between the dry season water potential (P_{min}) and P_{50} (HSM_{50}) or P_{88} (HSM_{88}. Thus, HSMs can contextualize plant water potentials relative to a species' vulnerability to embolism (Powers *et al.*, 2020; Skelton *et al.*, 2021; Tavares *et al.*, 2023).

Embolism resistance and hydraulic efficiency are thought to be linked to xylem anatomy. Wider, longer conduits that conduct water more efficiently than narrower, shorter ones are thought to have fewer conduit end walls where hydraulic resistance can increase tension and drive embolism spread, suggesting a mechanistic tradeoff between safety and efficiency (Hacke *et al.*, 2006; Christman *et al.*, 2012; Tyree & Zimmermann, 2013; Guet *et al.*, 2015; Gleason *et al.*, 2016; Levionnois *et al.*, 2021). However, embolism resistance may not be directly related to conduit diameter (Volaire *et al.*, 2018; Trueba *et al.*, 2019; Avila *et al.*, 2022; Jiang *et al.*, 2022; Lens *et al.*, 2022). As a result, the safety-efficiency tradeoff may be

weak (Gleason *et al.*, 2016) or depend on the range of trait values covered and the level of data aggregation (Isasa *et al.*, 2023). However, the relationship between conduit diameter and vulnerability is complex and may depend on the 3D topology of the conduit network, the proportions of vessels and tracheids, and nano-scale xylem traits (Lens *et al.*, 2023; Olson *et al.*, 2023; Pratt *et al.*, 2023).

Interconduit pits, which connect adjacent conduits, have also been thought to influence embolism spread through the xylem network. Interconduit pits may function either as safety valves that close under tension and prevent embolism spread or as pores that optimize hydraulic conductance of the xylem network by reducing hydraulic resistance between adjacent conduits (Kaack *et al.*, 2021). Pits may represent ~50% of the total plant hydraulic resistance (Sperry *et al.*, 2005; Hacke *et al.*, 2006; Choat *et al.*, 2008; Jacobsen & Pratt, 2018; Kaack *et al.*, 2019). Thus, pit ultrastructure may influence both safety and efficiency by limiting embolism spread during drought while also allowing for water flow between adjacent conduits (Pittermann *et al.*, 2005; Choat *et al.*, 2008; Tyree & Zimmermann, 2013). Functionally important pit traits include the thickness of the interconduit pit membranes leading to narrower pit membrane pores in flowering plants (Lens *et al.*, 2011), and the frequency of inter-conduit pits (Hargrave *et al.*, 1994). Thicker pit membranes reduce the likelihood of an air bubble traversing the pit membrane to spread into adjacent conduits. Pit frequency may influence embolism vulnerability, and there may be a tradeoff between having numerous pits in order to promote hydraulic integration and having few pits to prevent embolism spread (Hargrave *et al.*, 1994; Choat *et al.*, 2004; Wheeler *et al.*, 2005; Hacke *et al.*, 2006). Thicker pit membranes in flowering plants (and gymnosperm species without a torus-margo pit membrane) are often associated with greater embolism resistance (Lens *et al.*, 2011; Li *et al.*, 2016; Doria *et al.*, 2019; Trueba *et al.*, 2019; Kaack *et al.*, 2021; Levionnois *et al.*, 2021), and embolism-resistant species may sometimes exhibit narrower and more elliptically shaped pits and pit apertures and shallower pit chambers (Hacke & Jansen, 2009; Lens *et al.*, 2011; Scholz *et al.*, 2013). Taken together, these relationships between pit traits and embolism vulnerability suggest that plants with lower pit density, larger pit membrane area, larger pit aperture area, and less elliptical pits may be associated with higher hydraulic conductivity and lower embolism resistance (Pittermann *et al.*, 2010; Lens *et al.*, 2011; Brodersen *et al.*, 2014; Jacobsen *et al.*, 2016). Yet, the mechanistic link among anatomical

traits, hydraulic efficiency, and embolism vulnerability is complex, with no data for cycads (Gleason *et al.*, 2016; Lens *et al.*, 2022).

Interestingly, although axial water transport occurs predominantly via tracheids in cycads, some cycad species also have vessels, which are thought to have been one of the key innovations allowing angiosperms to transport higher fluxes of water (Jacobsen, 2021). In theory, species with a higher proportion of tracheids would be more resistant to embolism spread than species with a higher percentage of vessels (Pratt *et al.*, 2023), though data for cycads is lacking. Moreover, cycad species tend to have homogenous pit membranes similar to those of angiosperms (Schneider *et al.*, 2007; Jacobsen, 2021; Pang *et al.*, 2023) and ferns (Carlquist & Schneider, 2007), but different from the torus-margo pits of most non-cycad gymnosperms (Pittermann *et al.*, 2005; Carlquist & Schneider, 2007; Choat *et al.*, 2008). While increasing torus is associated with higher embolism resistance among conifers (Bouche *et al.*, 2014), pit size and tracheid size also influence embolism resistance (Song *et al.*, 2022). Yet, some pit traits of cycads differ from those of other vascular plant lineages and are linked to native climate (Pang *et al.*, 2023). For example, cycads have interconduit pit membranes larger than those of ferns and angiosperms but smaller than those of non-cycad gymnosperms, and cycads native to mesic habitats have larger pit membranes and lower pit density (D_p) than xeric species (Pang *et al.*, 2023). These patterns suggest that pit traits may influence embolism vulnerability, which may, in turn, influence drought tolerance and habitat affinities.

Cycads are an excellent system in which to test xylem structure-function relationships because congeneric species are closely related, recently diverged, and exhibit high diversity in overall morphology (Stevenson *et al.*, 1996; Zhang *et al.*, 2015), habitat affinities (Whitelock, 2003), and leaf structure (Zhang *et al.*, 2015; Zhang *et al.*, 2017; Coiro *et al.*, 2020; Glos *et al.*, 2022; Coiro *et al.*, 2023). The unique morphology and smaller, less permeable pit membranes among cycads (Zhang *et al.*, 2015; Tomlinson *et al.*, 2018; Jacobsen, 2021; Pang *et al.*, 2023) suggest cycads may exhibit unique relationships among anatomical traits and embolism vulnerability. Additionally, the two cycad families differ ecologically in ways that may reflect differences in embolism vulnerability: Cycadaceae diversified earlier and occur in wetter habitats than Zamiaceae (Jiang *et al.*, 2016; Meng *et al.*, 2021; Coiro *et al.*, 2023). However, embolism vulnerability has not before been

169 quantified for cycads. Therefore, we asked: (1) How do embolism resistance and HSMs vary
170 among cycad clades compared to other plant lineages (angiosperms, pteridophytes, and non-
171 cycad gymnosperms)? (2) Are tracheid and vessel traits correlated with embolism
172 vulnerability and HSMs in cycad leaves? (3) Do pit traits of tracheids or vessels correlate
173 with hydraulic safety? To address these questions, we measured embolism vulnerability and
174 used light microscopy (LM), scanning electron microscopy (SEM), and transmission electron
175 microscopy (TEM) to quantify pit and tracheid traits among 20 cycad species (Fig. 1, Table
176 1). We also measured dry season midday water potentials to estimate the minimum seasonal
177 water potential (P_{min}) and pressure-volume (PV) curves to calculate hydraulic safety margins
178 (HSMs). We predicted that the long-lived, durable leaves of cycads would be highly resistant
179 to drought-induced embolism and that their variation in their vulnerability to embolism would
180 be linked to anatomical traits, such as interconduit pit frequency and thickness, which have
181 been shown to influence vulnerability to embolism spread in other plant groups.
182

183 **Materials and Methods**

184 **Plant material**

185 Three to five healthy individuals from each of ten Cycadaceae species and ten Zamiaceae
186 species, representing five of the ten cycad genera (Table 1), were sampled from the Nanning
187 Botanical Garden, Nanning, Guanxi Province, China (22°47′12.93″, 108°23′3.30″). Plants
188 were watered approximately weekly depending on precipitation. On each plant, one sun-
189 exposed rachis with intact pinnae was cut in the evening or early morning, sealed in a black
190 plastic bag with wet tissues, then transported to the laboratory within an hour. Rachises were
191 recut under water and allowed to rehydrate while covered with a black plastic bag for ~8
192 hours.

193 **Measurement of vulnerability curves**

194 The pneumatic method was used to estimate embolism vulnerability on rachises with intact
195 pinnae for all 20 species (Pereira *et al.*, 2016), based on our previous validation of the
196 pneumatic VCs with the bench-drying method for three cycad species (Qin *et al.*, 2022). We
197 used the Pneumatron device for automated measurements of air discharge (AD) using a
198 reservoir volume of 3.5 ml (Pereira *et al.*, 2020). The reservoir pressure was monitored by the
199 Pneumatron every 0.5 sec for one minute per measurement, with ten-minute intervals
200 between measurements.
201

202 The basipetal end of each fully hydrated rachis was cut in air with a sharp razor blade to clear
203 obstructions for air flow and then connected to the Pneumatron (Pereira *et al.*, 2016; Pereira
204 *et al.*, 2020). Because most species exude mucilage that clogs tubing, we recut the rachis to
205 remove accumulated mucilage periodically until no more mucilage was seen at the cut end.
206 During VC measurements, rachises with leaves were slowly dehydrated in a dark,
207 temperature-controlled room, allowing water potentials to remain equilibrated throughout the
208 measurements (Sperry *et al.*, 1988). The duration of the drydown for each sample varied from
209 8 to 30 days depending on the species. Periodically during this period, xylem water potentials
210 of pinnae were measured using a Scholander pressure chamber (0.01MPa resolution; PMS
211 Instrument Company, Albany, OR, USA). Prior to excising pinnae for water potential
212 measurement, pinnae were covered with aluminum foil and sealed in a plastic bag for at least
213 1 hour, so that they could equilibrate with the rachis water potential. Immediately after
214 excising the pinna, the cut surface on the rachis was sealed with a quick-drying adhesive to
215 prevent leakage during subsequent AD measurements (Pereira *et al.*, 2016). For each sample,
216 we made 9-10 water potential measurements throughout the duration of the AD
217 measurements. AD measurements were stopped when the rachises and pinnae had dehydrated
218 and no more air was discharged in at least 60 consecutive measurements. To match water
219 potential to AD, we assumed water potential declined linearly between consecutive water
220 potential measurements, allowing interpolation of water potential at every time point.
221
222 Most of the vulnerability curves exhibited two plateaus, with the first plateau representing
223 empty mucilage canals and the second plateau representing fully embolised conduits. The
224 percent of AD at each measurement (PAD_i) into the reservoir was calculated as (Pereira *et*
225 *al.*, 2016):
226
227 $$PAD_i = 100 * (AD_i - AD_{min}) / (AD_{max} - AD_{min})$$
228
229 where AD_i is the amount of air discharged for measurement i, AD_{min} is the minimum amount
230 of air discharged from the fully hydrated branch, and AD_{max} is the maximum amount of air
231 discharged from the branch when completely desiccated. PAD was plotted against water
232 potential and a logistic function used to estimate critical water potentials (Pammenter &
233 Vander Willigen, 1998):
234

235 $PAD = 100 / (1 + exp((S_p / 25)(P_x - P_{50})))$

236

237 where S_p (%PAD MPa^{-1}) is the slope of the curve. From this equation, the P_{12}, P_{50}, P_{88} were
238 calculated for PAD of 12%, 50%, 88%, respectively. Because measurement of gas discharge
239 before Ψ_{tlp} is affected by open conduits, we followed recent protocols to exclude water
240 potentials above Ψ_{tlp} (Miranda *et al.*, 2023).

241 **Light microscopy**

242 All measurements were made on one fully expanded, sun-exposed rachis with pinnae
243 sampled from each individual. Cross-sections of the rachis were made ~30 cm from the
244 rachis tip using a sliding microtome (RM225, Leica Inc.) at a thickness of 30-60 µm. Sections
245 were bleached for 10 min, rinsed in water, stained with Safranin O (0.5% w/v in water) for 5
246 min and Alcian Blue (1% w/v in 3% acetic acid) for 20 secs - 1 min, then mounted on glass
247 slides. Images of rachis cross-sections were taken at 5x and 10x, with fields of view of
248 approximately 3.99 mm^2 and 0.89 mm^2, respectively, using a compound microscope outfitted
249 with a digital camera (DM3000, Leica Inc.). About 50 - 80 images were taken for each rachis
250 and stitched together using Leica Application Suite (v.4.11; Switzerland). We measured
251 number of conduits (N), conduits density (T_d), long/short diameter of conduits, and double
252 conduit wall thickness (T_w) using ImageJ (Rueden *et al.*, 2017).

253 To determine tracheid length (L_t), we cut longitudinal rachis segments (~5 cm in length)
254 from the same rachis sampled for cross-sections into ~5-mm thick blocks and incubated them
255 at 70°C in a 1:1 solution of H_2O_2 (30%) and acetic acid (100%) until all pigments had been
256 removed. Blocks were removed from this solution, placed in a petri dish with water for 3-5
257 minutes, and flattened with forceps, allowing tracheids to be stained. All samples were
258 stained with Alcian Blue (1 % w/v in 3 % acetic acid) for 10 min, washed in water, mounted
259 on slides, and imaged at 5x. About 10-25 images were taken for each rachis sample and
260 stitched together. L_t of ~50 tracheids per species was measured from the stitched images
261 using ImageJ (Fig. 1).

262 **Pit characteristics from scanning electron microscopy (SEM) and transmission electron**
263 **microscopy (TEM)**

264 Freshly collected rachises were cut into 1-3 cm long pieces and placed in 100 ml 5% FAA
265 (90:5:5 ratio of 70% ethanol, acetic acid, formaldehyde) at room temperature (25°C) to
266 prevent expansion or shrinkage. Longitudinal sections ~1-cm long were made with a sliding
267 microtome at a thickness of 2-3 mm, fixed to aluminum sample holders with carbon double-

268 sided tape (Nisshin EM Co., Ltd.), air-dried for 12 h at room temperature, and coated with
269 gold using a sputter coater (Cressington 108Auto) for 40 secs at 0.08 mA under an argon
270 atmosphere to produce a 20-nm-thick gold layer. A scanning electron microscope (FEI
271 Quattro S) with a voltage of 2 kV was used to visualize inter-tracheid pits according to
272 standard protocols (Jansen *et al.*, 2009; Lens *et al.*, 2011). Mean values for all pit traits (Table
273 2) were based on at least 50 measurements from SEM images of various inter-tracheid walls
274 per plant.
275
276 Because vessels have been found in cycads (Huang & Zhang, 1999; Huang *et al.*, 2017;
277 Jacobsen, 2021), we examined maceration slides of all 20 species to identify vessel elements.
278 Because it is difficult to distinguish between tracheids and vessels in cross-section in cycads,
279 we estimated the proportions of tracheids and vessels from longitudinal sections of vascular
280 bundles imaged with SEM (Fig. 1). For a given area of interest (AOI), all vessel elements and
281 tracheids were measured for area, diameter and length. The percentage per image area of
282 vessels or tracheids was calculated as vessels (or tracheids) % = vessel areas (or tracheid
283 areas) / area of AOI x 100%.
284
285 For TEM measurements, ~1-cm long segments from the freshly collected rachis were cut into
286 1x2-mm blocks. These blocks were fixed within 10 min after sampling in 500 µl of buffered
287 glutaraldehyde (25% glutaraldehyde 3 ml, 0.2 mol sodium phosphate buffer 15 ml, ddH_2O 12
288 ml) for one night under a vacuum (~50 kPa). Samples were cleaned for 15 min under vacuum
289 with 0.1 mol NaH_2PO_4 buffer three times, transferred to a 1% $KMnO_4$ solution for 1-h under
290 vacuum, then cleaned again under vacuum for 15-min in 0.1 mol NaH_2PO_4 buffer three times.
291 Samples were then moved through an ethanol dehydration series with ~10 min per step (30%,
292 50%, 70%, 90%, and 100%), followed by another 20-min dehydration in 100% acetone
293 100%. Samples were then moved through an acetone (100%): Epon resin (Pelco; Epon resin:
294 Dodecenyl succinic anhydride: Methyl Nadic 8:3:5) dilution series: 5-h in a 3:1 acetone:Epon
295 resin, 5-h in 1:1 acetone:Epon resin, and 12-h in 1:3 acetone:Epon resin. Samples were then
296 transferred to 100% Epon resin (Pelco; Eponate 12 resin: Dodecenyl succinic anhydride:
297 Methyl Nadic 8:3:5) for 12-h and heated at 37°C, 45°C, and 60°C for 12-h, 12-h, and 48-h,
298 respectively, to polymerize the resin. All these steps occurred under the same vacuum
299 conditions.
300

With an ultra-microtome (Leica Ultracut EMUC7/FC7, Leica Inc.) 50-90 nm thick sections were cut and placed on copper grids (Athena, Plano GmbH, Wetzlar, Germany). Samples were stained in the dark with 1% uranyl acetate and 1% lead citrate for 10 min. We used a transmission electron microscope (HT-7700, Hitachi, Japan) at an acceleration voltage of 80 kV and 18 mA to obtain digital images based on at least one cross-section of a rachis per individual and three individuals per species. Pit membrane thickness (T_{pm}) and pit chamber depth (D_{pc}) were measured on ~50 interconduit pit membranes obtained from 3-5 sections per species using ImageJ.

Hydraulic safety margins (HSMs)

Midday leaf water potentials (P_{min}) were measured between 12:30–14:00 h in the peak of the dry season on consecutive sunny days and repeated for all species in years 2020, 2021, and 2022. For each species, 3-5 sun exposed rachises from different individuals were excised and sealed in humidified plastic bags ~2 hr to allow water potential equilibration. Leaf water potential was measured by inserting one pinna into a Scholander-style pressure chamber. We took P_{min} (mean values of three individuals) to be the most negative of the three measurements during the three years. Hydraulic safety margins were calculated from P_{min} and VCs as $HSM_{50} = P_{min} - P_{50}$ and $HSM_{88} = P_{min} - P_{88}$.

Pressure–volume curves

Shoots with leaf pinnae were collected from at least three individuals per species at night or at predawn and transported back to the laboratory, then recut underwater and allowed to rehydrate for at least 6-h while covered with a black plastic bag. Initial water potentials of leaf pinnae were always close to -0.2 MPa. Pressure–volume curves were constructed for each sample by repeatedly measuring bulk water potential using a pressure chamber and weighing the sample mass (±0.0001g, model ML204T; Mettler Toledo) to determine the relationship between water potential and water content (Scholander *et al.*, 1965; Sack & Pasquet-Kok, 2011; Roddy *et al.*, 2019; Jiang *et al.*, 2022). Prior to each water potential measurement, samples were equilibrated in humidified plastic bags for ~20 min. The pressure chamber was kept humidified with wet paper towels to prevent evaporation during measurement. At the end of measurements, pinna area was measured using a LI-3000A leaf area meter (Li-Cor) and the sample was oven-dried at 70 °C for at least 72-h before determining dry mass. From these curves, we calculated saturated water content (SWC),

absolute capacitance (C_T), water potential at turgor loss point (Ψ_{tlp}), and water content at the turgor loss point (RWC_{tlp}), as well as leaf mass per area (LMA) (Table 2).

Data analysis

All statistical analyses were performed using R (version 4.1.3, R Development Core Team). We used linear regression and standard major axis (SMA) regression (R package 'smatr') to determine the relationships between traits (Warton *et al.*, 2012), and the statistical tests were considered significant at P <0.05. Principal component analysis (PCA) was carried out using the 'vegan' package. Mean trait values were z-scaled and centered prior to calculating principal components, and we removed strongly correlated traits with similar functional implications to prevent having more traits than the number of taxa. Correlations among P_{12}, P_{50}, P_{88}, HSM_{50}, HSM_{88}, and the PC1 and PC2 scores were tested with Pearson correlations. Differences among cycads and other plant lineages were analyzed using one-way ANOVA, followed by Tukey post-hoc tests. Student's *t*-tests were used to determine differences in traits between Cycadaceae and Zamiaceae. Published data for P_{12}, P_{50}, P_{88}, HSM_{50}, HSM_{88}, D_h, and L_t of other vascular plant groups were obtained from https://xylemfunctionaltraits.org/. Because only one species of non-cycad gymnosperm had data for leaves, this comparison necessarily was between primary xylem in cycad rachises and primary and secondary xylem in woody species of gymnosperms and angiosperms, which included stems and leaves. Data for most of ferns were from (Suissa & Friedman, 2021) and (Pittermann *et al.*, 2011) using WebPlotDigitizer.

In addition to PCA, we also used Canonical Correlation Analysis (CCA) to determine whether there were correlations between suites of traits. For CCA, we used four groups of traits: pressure-volume traits (SWC, C_T, Ψ_{tlp}, RWC_{tlp}), vessel traits (vessel proportion, vessel diameter, hydraulic weighted vessel diameter D_v, L_v, vessel F_{pf}, vessel A_{pit}, vessel R_{pit}, vessel D_p, and T_{pm}), tracheid traits (tracheid proportion, A_{pit}, A_{pa}, A_p, F_{pf}, F_{pa}, R_{pit}, R_{pa}, D_p, T_{pm}, D_t, CWR, L_t), and vulnerability traits (P_{min}, P_{12}, P_{50}, P_{88}). We used log-transformed traits and the R packages 'CCA' and 'CCP' to run analyses and test for significant relationships using the Wilks' Lambda approximation of the F-statistic.

To account for the statistical non-independence of species with shared evolutionary history, we incorporated phylogenetic covariance into our regression analyses. We pruned the phylogenetic tree from (Coiro *et al.*, 2023) to include only our 20 species. We calculated

365 phylogenetically corrected generalized least squares regressions for pairwise trait
366 combinations using the R packages "ape" (Paradis & Schliep, 2018), "caper" (Orme *et al.*,
367 2012), and "phytools" (Revell, 2012) with functions of "read.tree", "dplyr",
368 "comparative.data", "nlme", and "gls" with "corBrownian" correlation structure.
369

370 **Results**

371

372 **Hydraulic safety of cycads**

373 Most of the pneumatic non-adjusted VCs were sigmoid in shape (Fig. S1), some species
374 exhibited substantial variation in VCs among individuals (e.g. *E. manikensis*, *C.*
375 *segmentifida*, *Z. furfuracea*) (Fig. 2) after adjusting them for gas discharge prior to turgor
376 loss. Adjusting curves had little effect on P_{12}, P_{50}, and P_{88} (Fig. 2), though adjustment shifted
377 the P_{12} significantly from -1.51 ± 0.12 in the non-adjusted curves to -1.95 ± 0.12 MPa ($P <$
378 0.05) in the adjusted curves. Across all 20 species, mean values of P_{12}, P_{50}, and P_{88} were -1.95
379 ± 0.12 MPa, -2.26 ± 0.15 MPa, -2.57 ± 0.21 MPa, respectively (Table 3). P_{12} of cycads was
380 similar to angiosperms, but more negative than pteridophytes, and non-cycad gymnosperms
381 had the most negative P_{12} (Table 3). P_{50} of cycads was similar to angiosperms and
382 pteridophytes, while non-cycad gymnosperms had the most negative values (Fig. 3a; Table
383 3). No differences in P_{88} were found between cycads and pteridophytes, but angiosperms and
384 non-cycad gymnosperms had more negative P_{88} than cycads (Fig. 3b; Table 3). Hydraulic
385 safety margins (HSM_{50}) of cycads were similar to pteridophytes and angiosperms, but non-
386 cycad gymnosperms had the highest values (Fig. S2; Table 3). HSM_{88} of cycads were also
387 similar to pteridophytes and angiosperms, non-cycad gymnosperms had the highest HSM_{88}
388 and pteridophytes the lowest values (Fig. S2; Table 3). P_{12}, P_{50}, and P_{88} were significantly
389 more negative among Cycadaceae than among Zamiaceae, but these differences were not
390 reflected in HSM_{50} and HSM_{88} because P_{min} was also more negative among Cycadaceae than
391 Zamiaceae (Table S1).
392

393 Vessels were found in all 20 cycad species (Fig. 1; S3), but the proportions of vessels were
394 relatively low compared to proportion of tracheids (Table 4), and vessel diameter (D_v) was
395 similar as tracheid diameter (D_t), L_t was much longer than vessel element (L_v) (Table 4).
396 Tracheid diameters (D_t) of cycads were significantly narrower than those of angiosperms,

397 similar to pteridophytes and non-cycad gymnosperms (Fig. S4a; Table 3), but cycads had
398 significantly longer L_t than non-cycad gymnosperms (Fig. S4b; Table 3), similar to ferns.
399

400 **Trait-by-trait relationships**

401 Overall, there were few significant correlations between anatomy and physiology among
402 cycads for the traits measured here. No pairwise correlations between metrics of vulnerability
403 to embolism (P_{12}, P_{50}, P_{88}) and either tracheid and vessel traits (D_t, L_t, CWR, D_v, L_v) or pit
404 membrane thickness (T_{pm}) and depth of the pit chamber (D_{pc}) were significant (Fig. 4; Fig.
405 S5), even after accounting for shared evolutionary history (Table S2, S3). P_{12}, P_{50}, P_{88}, and
406 HSM_{50} also showed no correlations to pit density (D_p), pit membrane shape (R_{pit}) of vessels or
407 tracheids, except that P_{50} and P_{88} were negatively correlated with R_{pit} of tracheids (Fig. S6).
408 However, the relationship between HSM_{50} and tracheid D_p became significant after
409 accounting for shared evolutionary history (Table S2). Only the longest pit aperture axis
410 (D_{pal}) and pit aperture shape (R_{pa}) of tracheids were correlated with metrics of vulnerability
411 (Fig. S7; Table S2, S3), though these became non-significant after accounting for shared
412 evolutionary history (Table S2). P_{12}, P_{50}, P_{88}, HSM_{50}, and HSM_{88} showed no correlations to
413 vessel or tracheid proportions, except that tracheid proportion was positively correlated with
414 HSM_{50} (Fig. 5), though this correlation was weakened after accounting for shared
415 evolutionary history ($P = 0.0506$) (Table S2). However, P_{12}, P_{50}, P_{88}, HSM_{50}, and HSM_{88} were
416 significantly correlated with pit membrane fraction (F_{pf}) and pit membrane size (A_{pit}) of
417 vessels but not of tracheids (Fig. 6; Table S2, S3).
418

419 The two cycad families displayed significant differences in average trait values. Zamiaceae
420 had significantly shorter D_{pms}, smaller A_{pit}, and lower F_{pf} of vessels than Cycadaceae, as well as
421 longer D_{pal}, higher F_{pa}, more elliptical pit (R_{pit}) and pit aperture (R_{pa}) shapes, thinner pit
422 membranes (T_{pm}), and higher density of conduits than Cycadaceae (Table S4). Turgor loss
423 points (Ψ_{tlp}) were significantly less negative in Zamiaceae than in Cycadaceae, and
424 Zamiaceae had higher LMA (Table S5). Interestingly, Ψ_{tlp} was significantly correlated with
425 P_{min}, P_{12}, P_{50}, and P_{88}, even after accounting for shared evolutionary history (Fig. 7; Table S2).
426

427 **Multivariate analyses**

428 CCA revealed a significant correlation between the suite of embolism vulnerability traits and
429 the suite of vessel traits. The first two dimensions of the CCA were significant, with

canonical correlations of 0.96 ($\lambda = 0.003$, F = 2.93, df = 36, P = 0.002) and 0.91 ($\lambda = 0.038$, F = 2.06, df = 24, P = 0.04). The first canonical dimension was most strongly correlated with vessel D_p (0.47) and T_{pm} (0.37) versus vessel proportion (-0.44), D_v (-0.44), and vessel R_{pit} (-0.29). The second canonical dimension was most strongly influenced by vessel F_{pf} (0.72) and vessel A_{pit} (0.57) versus vessel diameter (-0.13), vessel proportion (-0.13), and vessel D_p (-0.13) (Fig. 8, S8; Table 5-6). No other canonical correlations (e.g. tracheid traits vs. vulnerability, tracheid traits vs. PV traits, vessel traits vs. PV traits, PV traits vs. vulnerability) between suites of traits were significant.

PCA using species' z-scaled and centered trait values for the 22 pit, tracheid, vessel, and PV traits (Table 2) revealed that the first two components explained 21.91% and 15. 58% of the total variation, respectively (Fig. S9). The first PC was driven mainly by both tracheid and vessel traits of R_{pit}, R_{pa}, F_{pf}, D_{pc}, T_{pm}, A_{pit}, D_p, and RWC_{tlp}, LMA, Ψ_{tlp} (Fig. S9). The second PC was most strongly associated with A_{pa}, T_{pm}, D_t, CWR, and L_v (Fig. S9). Vulnerability traits P_{12}, P_{50}, P_{88}, HSM_{50}, and HSM_{88} showed no correlations with PC2 scores (Table S6). On the other hand, HSM_{50} and HSM_{88} were positively associated with PC1 scores, driven primarily by R_{pit} and R_{pa} of tracheids, T_{pm} and D_{pc}, and F_{pf}, A_{pit} of vessels, as well as LMA and Ψ_{tlp} (Fig.S9; Table S6).

Discussion

Despite their ecological and evolutionary importance, cycads have been largely overlooked in studies of plant water relations and hydraulics. Cycads started to prosper during the Carboniferous (Coiro *et al.*, 2023), a period of global drying that culminated in terrestrial biodiversity loss during the Carboniferous rainforest collapse (Sahney *et al.*, 2010). Such dramatic climate change is often a strong agent of selection, such that lineages diversifying during these time periods often show signs of adaptive changes in morphology, anatomy, and physiology (Crane *et al.*, 1995; Pittermann *et al.*, 2012; Condamine *et al.*, 2015; Simonin & Roddy, 2018). Furthermore, extant cycads occur naturally across a range of habitats in tropical and subtropical regions (Calonje *et al.*, 2022). These aspects of cycad ecology and evolutionary history would suggest that cycads would be drought-tolerant. Yet, our results show that cycads are more vulnerable to drought-induced embolism than most other gymnosperms.

463 **Embolism resistance, safety margins, and water relations of cycads**

464 Given the diversification history and ecology of extant cycads, we had predicted cycads
465 would be at least as resistant to embolism as other gymnosperms. However, our results
466 showed that cycads had more vulnerable P_{50} than non-cycad gymnosperms (Fig. 3; Table 3).
467 This pattern could be due to our comparison of cycad rachises to gymnosperm stems, even
468 though cycad leaves are long-lived, or to cycads' relying on drought resistance traits other
469 than only embolism resistance. For example, cycads have large, pachycaulous stems, large
470 rachises with mucilage, and thick leaflets, all of which may allow for high water and
471 carbohydrate storage that can prolong survival and delay water potential declines during
472 protracted droughts (Marler, 2023). However, HSMs of cycads were as low as in other major
473 plant groups, indicating that cycad water potentials frequently approach turgor loss and
474 embolism spread, increasing their risk of hydraulic failure (Choat *et al.*, 2012; Brodribb *et al.*,
475 2020). These low HSMs in cycads occurred even in plants that were regularly watered,
476 suggesting that cycads may always operate near thresholds of turgor loss and embolism
477 spread (Fig. 7). Because high HSM_{50} can be a strong predictor of biomass accumulation
478 (Tavares *et al.*, 2023), low HSM_{50} among cycads may play a role in their slow rates of growth
479 and biomass accumulation. The low margin of turgor loss, high vulnerability to embolism
480 spread, and low hydraulic safety margins together suggest that cycads have a limited range of
481 operational water potentials and that physiological drought may quickly impede
482 photosynthetic carbon uptake.
483

484 Many other cycad traits are consistent with a physiological strategy characterized by low
485 rates of metabolism. Cycads exhibit high LMA and low SWC and hydraulic capacitance (C_T),
486 both of which are on the low end for angiosperm leaves (Table S5) (Roddy *et al.*, 2019; An *et*
487 *al.*, 2023), all trait values consistent with low rates of photosynthetic metabolism (Wright *et*
488 *al.*, 2004; Zhang *et al.*, 2015; Wang *et al.*, 2022; Nadal *et al.*, 2023). Yet, they benefit from
489 symbiotic nitrogen-fixing cyanobacteria (Kipp *et al.*, 2023), which may elevate their water
490 use efficiency and potentially compensate for the limiting effects of low SWC on metabolic
491 rates (Wang *et al.*, 2022). While high hydraulic capacitance can forestall water potential
492 declines (Smith-Martin *et al.*, 2022), particularly in species with high vulnerability to
493 embolism spread, cycads were both highly vulnerable to embolism and had low leaf
494 hydraulic capacitance. Yet, in our bench-drying experiments to measure embolism
495 vulnerability, shoots required 8-30 days to desiccate, suggesting that they may have low rates

496 of residual water loss, which is thought to be an important drought tolerance trait (Duursma *et*
497 *al.*, 2019; Roddy *et al.*, 2023). Together, these lines of evidence suggest that limiting water
498 loss through low rates of gas exchange and low residual conductance and high water storage
499 stem capacitance as Joshua tree (Simpson, 1975) may be important to cycad drought
500 resistance and may compensate for xylem that is vulnerable to embolism spread.
501

502 There were distinct differences in physiological traits between the two cycad families (Tables
503 S1, and S4-5). That Cycadaceae had more negative P_{min} and Ψ_{tlp} than Zamiaceae suggests that
504 these two families may be diverging along the isohydric-anisohydric axis (Tardieu &
505 Simonneau, 1998; McDowell *et al.*, 2008) (Table S1, S5; Fig. 7). That Zamiaceae may be
506 more isohydric than Cycadaceae is, perhaps, surprising given that Zamiaceae tend to occur in
507 drier habitats than Cycadaceae (Meng *et al.*, 2021). Notably, the species we sampled include
508 some of the more mesic species of *Encephalartos* and do not include *Dioon*, which is thought
509 to be drought-tolerant, suggesting that the differences between families observed here may be
510 due, in part, to a sampling bias. More evidence is needed to further characterize these
511 hydraulic strategies and how they may be linked to climate preferences. More generally,
512 conifer species differing in their degree of isohydry vs. anisohydry exhibit different stomatal
513 behaviors mediated by abscisic acid concentrations (Brodribb *et al.*, 2014), but work on
514 stomatal physiology in cycads has been limited (Haworth *et al.*, 2011).
515

516 **Correlations between embolism resistance and anatomy**

517 A variety of xylem traits have been posited as determinants of embolism resistance, including
518 conduit dimensions, xylem network structure, frequency of interconduits pits, and the
519 ultrastructure of interconduit pits and their membranes (Kaack *et al.*, 2021; Lens *et al.*, 2022;
520 Pereira *et al.*, 2023). Our measurements suggest that vessel but not tracheid was likely linked
521 to vulnerability to embolism spread among cycads. Xylem conduit dimensions have long
522 been thought to influence both hydraulic efficiency and safety (Hargrave *et al.*, 1994;
523 Christman *et al.*, 2012; Guet *et al.*, 2015; Levionnois *et al.*, 2021). Cycads exhibited wider
524 conduit and longer tracheids (L_t) than other non-cycad gymnosperms (Fig. S4; Table 3), both
525 of which would lead to higher hydraulic conductivity per conduit and greater embolism
526 vulnerability. However, embolism resistance among cycads was unrelated to conduit traits,
527 including tracheid and vessel dimensions and tracheid cell wall reinforcement (Fig. 4-5),
528 consistent with data for ferns (Pittermann *et al.*, 2011), but in contrast to data for conifer

529 stems (Song *et al*., 2022). Though larger xylem conduits have been thought to confer greater
530 embolism vulnerability (Pittermann *et al.*, 2006; Gleason *et al.*, 2016), many studies have
531 failed to find relationships between conduit dimensions and embolism vulnerability in a
532 variety of taxa, now including cycads (Volaire *et al.*, 2018; Trueba *et al.*, 2019; Avila *et al.*,
533 2022; Jiang *et al.*, 2022). Notably, for cycads studied here, we investigated the relationships
534 in primary xylem which might be different from the secondary xylem in other plant taxa.
535 Cycads had longer and wider tracheids than other gymnosperms as ferns (Pittermann *et al.*,
536 2011), which would increase their hydraulic efficiency and potentially allow for higher rates
537 of water transport and competitive ability.

538

539 The frequency of interconduit pits may also influence embolism spread. Wider conduits
540 would have more interconduit pits because they have more surface area even if the frequency
541 of pits on the conduit surface were constant. Since embolism spread needs only one pit, more
542 pits would increase the likelihood of embolism spread between adjacent conduits (Hargrave
543 *et al.*, 1994; Choat *et al.*, 2004). Similarly, a higher pit frequency on the conduit surface (i.e.
544 higher F_{pf}) would also increase the total number of pits on a conduit and the likelihood of
545 embolism spread (Wheeler *et al.*, 2005; Hacke *et al.*, 2006). However, cycads exhibited no
546 significant relationships between embolism resistance and tracheid traits (tracheid diameter
547 and length, interconduit pit area A_{pit}, density, and fraction F_{pf}) (Fig. S6, S10; Table S2).
548 However, higher F_{pf} and A_{pit} of vessels were associated higher embolism resistance (Fig.6;
549 Table S3), notably in contrast to predictions (Lens *et al.*, 2023; Pratt *et al.*, 2023).

550

551 The structure of pit membranes may also influence embolism resistance. Because pit
552 membranes are composed of layers of crossing fibers, an air bubble must be pulled through
553 the pores of the pit membrane in order to move between connected conduits. Thin pit
554 membranes are more likely to have larger pores than thicker pit membranes, providing an
555 explanation for why pit membrane thickness is a good predictor of embolism resistance (Lens
556 *et al.*, 2011; Doria *et al.*, 2019; Trueba *et al.*, 2019; Kaack *et al.*, 2021; Levionnois *et al.*,
557 2021). However, among cycads there was no correlation between pit membrane thickness and
558 embolism vulnerability (Fig. S5). Rather, tracheid pit shape and pit aperture shape were
559 correlated with P_{50} and P_{88} (Figs.S6-7; Table S2) and have been shown to also correlate with
560 native climate among cycads (Pang *et al.*, 2023).

These results suggest that embolism resistance in cycads may be due to complex relationships among anatomical traits. The CCA results revealed that xylem vessel traits and vulnerability were related in the first two dimensions, with higher T_{pm}, vessel D_p, vessel F_{pf}, and vessel A_{pit} being most strongly associated with more negative P_{min}, P_{12}, P_{50}, and P_{88} (Fig. 8, S8; Tables 5-6). That T_{pm} and vessel D_p emerged as important traits in the CCA but exhibited no significant pairwise relationship with any critical water potential highlights that relationships among anatomical traits may be more important than any single trait. Though some angiosperms exhibit strong relationships between a single anatomical trait and embolism vulnerability (Lens *et al.*, 2011; Li *et al.*, 2016; Doria *et al.*, 2019; Trueba *et al.*, 2019; Kaack *et al.*, 2021; Levionnois *et al.*, 2021), our results highlight that embolism vulnerability is likely influenced by complex interactions among multiple traits (Pittermann *et al.*, 2021; Lens *et al.*, 2023). If changes in one trait are easier to evolve than changes in multiple traits, then our results suggest that cycads may be less adaptable to climate change than angiosperms. Alternatively, if small changes to many traits are easier to evolve than large changes to a single trait, then cycad physiology may be more adaptable than that of angiosperms.

Conclusion

Cycads provide an excellent opportunity to understand the evolutionary history of xylem structure-function relationships. All cycads studied here had vessels and were consistently more vulnerable to embolism with narrower hydraulic safety margins than other gymnosperms. Furthermore, many of the xylem traits thought to influence embolism resistance in other plant groups revealed no significant correlations with embolism resistance among cycads. Rather, the anatomical determinants of embolism resistance among cycads may depend on the many interactions between these anatomical traits, especially vessel traits. Differences in embolism resistance and xylem anatomy between the two extant cycad families suggest species in these two families may employ divergent physiological strategies to cope with drought. Although cycads have declined in dominance since their peak prior to the Cretaceous angiosperm revolution, their rapid and recent diversification in the face of aridification suggests that physiological and anatomical evolution may have been an important axis of evolution (Crane *et al.*, 1995; Condamine *et al.*, 2015; Simonin & Roddy, 2018). Understanding these ecophysiological strategies and tolerance may prove crucial in

conserving the ~70% of extant cycads that are currently endangered and in predicting their responses to future climate change.

Acknowledgements

We thank the Nanning Botanical Garden, for providing access to plants and help in field sampling. We thank F. Lens, J. Pittermann, and two anonymous reviewers for useful comments on the manuscript. We also gratefully thank the core facility center of State Key Laboratory for Conservation and Utilization of Subtropical Agro-Bioresources for providing technical supports. This work was supported by grants from the Natural Science Foundation of Guangxi Province (Key Program 2022GXNSFDA035059), and the Bama county program for talents in science and technology, Guangxi, China (20210020, 20220011) to G-FJ., and the Scientific Research Project of Qingxiu Mountain Management Committee (QXS2021-05). ABR was supported by US National Science Foundation grant number IOS-2243971.

Author contributions

G.-F.J. conceived the ideas and designed the study. G.-F.J., B.-T.Q., Y.-K.P., and L.-L.Q. collected the data. G.-F.J., B.-T.Q., Y.-K.P., L.-L.Q., L.P., and A.B. R. analyzed the data. G.-F.J. wrote the manuscript, and all authors reviewed and revised each draft before giving approval for submission of the final version.

Competing interests

None declared.

Data availability

All data supporting the findings of this study are available within the paper and within its supplementary data published online. Reuse of the data is permitted after obtaining permission from the corresponding author.

References

Adams HD, Zeppel MJB, Anderegg WRL, Hartmann H, Landhausser SM, Tissue DT, Huxman TE, Hudson PJ, Franz TE, Allen CD, et al. 2017. A multi-species synthesis of physiological mechanisms in drought-induced tree mortality. *Nature Ecology & Evolution* **1**(9): 1285-1291.

An YD, Roddy AB, Zhang TH, Jiang GF. 2023. Hydraulic differences between flowers and leaves are driven primarily by pressure-volume traits and water loss. *Frontiers in Plant Science* **14**: 1130724.

Avila RT, Kane CN, Batz TA, Trabi C, Damatta FM, Jansen S, McAdam SAM. 2022. The relative area of vessels in xylem correlates with stem embolism resistance within and between genera. *Tree physiology*.

Bouche PS, Larter M, Domec JC, Burlett R, Gasson P, Jansen S, Delzon S. 2014. A broad survey of hydraulic and mechanical safety in the xylem of conifers. *J Exp Bot* **65**(15): 4419-4431.

Bouda M, Huggett BA, Prats KA, Wason JW, Wilson JP, Brodersen CR. 2022. Hydraulic failure as a primary driver of xylem network evolution in early vascular plants. *Science* **378**(6620): 642-646.

Brenner ED, Stevenson DW, Twigg RW. 2003. Cycads: evolutionary innovations and the role of plant-derived neurotoxins. *Trends Plant Sci* **8**(9): 446-452.

Brodersen C, Choat B, Jansen S, Rico C, Pittermann J. 2014. Cavitation Resistance in Seedless Vascular Plants: The Structure and Function of Interconduit Pit Membranes. *Plant physiology* **165**.

Brodersen CR, Roddy AB, Wason JW, McElrone AJ. 2019. Functional Status of Xylem Through Time. *Annual Review of Plant Biology* **70**: 407-433.

Brodribb TJ, McAdam SA, Jordan GJ, Martins SC. 2014. Conifer species adapt to low-rainfall climates by following one of two divergent pathways. *Proc Natl Acad Sci U S A* **111**(40): 14489-14493.

Brodribb TJ, Powers J, Cochard H, Choat B. 2020. Hanging by a thread? Forests and drought. *Science* **368**(6488): 261-266.

Calonje M, Stevenson DW, Osborne R. 2022. The World List of Cycads, online edition [Internet]. *Available from: http://www.cycadlist.org*. .

Carlquist S, Schneider EL. 2007. Tracheary elements in ferns: New techniques, observations, and concepts. *American Fern Journal* **97**(4): 199-211.

Choat B, Brodribb TJ, Brodersen CR, Duursma RA, López R, Medlyn BE. 2018. Triggers of tree mortality under drought. *Nature* **558**: 531-539.

Choat B, Cobb AR, Jansen S. 2008. Structure and function of bordered pits: new discoveries and impacts on whole□plant hydraulic function. *New Phytologist* **177**(3): 608-626.

Choat B, Jansen S, Brodribb TJ, Cochard H, Delzon S, Bhaskar R, Bucci SJ, Feild TS, Gleason SM, Hacke UG, et al. 2012. Global convergence in the vulnerability of forests to drought. *Nature* **491**(7426): 752-755.

Choat B, Jansen S, Zwieniecki MA, Smets E, Holbrook NM. 2004. Changes in pit membrane porosity due to deflection and stretching: the role of vestured pits. *J Exp Bot* **55**(402): 1569-1575.

Christman MA, Sperry JS, Smith DD. 2012. Rare pits, large vessels and extreme vulnerability to cavitation in a ring-porous tree species. *New Phytol* **193**(3): 713-720.

Coiro M, Allio R, Mazet N, Seyfullah LJ, Condamine FL. 2023. Reconciling fossils with phylogenies reveals the origin and macroevolutionary processes explaining the global cycad biodiversity. *New Phytol*.

Coiro M, Jelmini N, Neuenschwander H, Calonje MA, Vovides AP, Mickle JE, Lumaga MRB. 2020. Evolutionary Signal of Leaflet Anatomy in the Zamiaceae. *International Journal of Plant Sciences* **181**(7): 697-715.

Condamine FL, Nagalingum NS, Marshall CR, Morlon H. 2015. Origin and diversification of living cycads: a cautionary tale on the impact of the branching process prior in Bayesian molecular dating. *BMC Evolutionary Biology* **15**: 65.

Crane PR, Friis EM, Pedersen KR. 1995. The origin and early diversification of angiosperms. *Nature* **374**(6517): 27.

Doria LC, Meijs C, Podadera DS, Del Arco M, Smets E, Delzon S, Lens F. 2019. Embolism resistance in stems of herbaceous Brassicaceae and Asteraceae is linked to differences in woodiness and precipitation. *Ann Bot* **124**(1): 1-14.

Duursma RA, Blackman CJ, Lopéz R, Martin-StPaul NK, Cochard H, Medlyn BE. 2019. On the minimum leaf conductance: its role in models of plant water use, and ecological and environmental controls. *New Phytologist* **221**(2): 693-705.

Gleason SM, Westoby M, Jansen S, Choat B, Hacke UG, Pratt RB, Bhaskar R, Brodribb TJ, Bucci SJ, Cao KF. 2016. Weak tradeoff between xylem safety and xylem□specific hydraulic efficiency across the world's woody plant species. *New Phytologist* **209**(1): 123-136.

Glos RAE, Salzman S, Calonje M, Vovides AP, Coiro M, Gandolfo MA, Specht CD. 2022. Leaflet Anatomical Diversity in Zamia (Cycadales: Zamiaceae) Shows Little Correlation with Phylogeny and Climate. *The Botanical Review*.

Guet J, Fichot R, Ledee C, Laurans F, Cochard H, Delzon S, Bastien C, Brignolas F. 2015. Stem xylem resistance to cavitation is related to xylem structure but not to growth and water-use efficiency at the within-population level in *Populus nigra* L. *J Exp Bot* **66**(15): 4643-4652.

Hacke UG, Jansen S. 2009. Embolism resistance of three boreal conifer species varies with pit structure. *New Phytologist* **182**(3): 675-686.

Hacke UG, Sperry JS, Wheeler JK, Castro L. 2006. Scaling of angiosperm xylem structure with safety and efficiency. *Tree physiology* **26**(6): 689-701.

Hargrave KR, Kolb KJ, Ewers FW, Davis SD. 1994. Conduit diameter and drought□induced embolism in Salvia mellifera Greene (Labiatae). *New Phytologist* **126**(4): 695-705.

Haworth M, Fitzgerald A, McElwain JC. 2011. Cycads show no stomatal-density and index response to elevated carbon dioxide and subambient oxygen. *Australian journal of botany* **59**(7): 630-639.

Hill KD, Stevenson DW, Osborne R. 2004. The world list of cycads. *The Botanical Review* **70**(2): 274-298.

Huang Y, Han Y, Wei L, Wang J. 2017. Comparative Studies of Tracheary Element Structure of Some Gymnosperms with Angiosperms. *American Journal of Plant Sciences* **08**: 959-984.

Huang YY, Zhang HD. 1999. The brief report on first discovery of vessel in cycads. *Journal of Guangxi Agricultural and Biological Science* **18**(2): 161-162.

Isasa E, Link RM, Jansen S, Tezeh FR, Kaack L, Sarmento Cabral J, Schuldt B. 2023. Addressing controversies in the xylem embolism resistance–vessel diameter relationship. *New Phytologist* **238**(1): 283-296.

IUCN. 2022. The IUCN Red List of Threatened Species. Version 2022-1. <https://www.iucnredlist.org>.

Jacobsen AL. 2021. Diversity in conduit and pit structure among extant gymnosperm taxa. *American Journal of Botany* **108**(4): 559-570.

Jacobsen AL, Pratt RB. 2018. Going with the flow: Structural determinants of vascular tissue transport efficiency and safety. *Plant Cell Environment* **41**(12): 2715-2717.

Jacobsen AL, Tobin MF, Toschi HS, Percolla MI, Pratt RB. 2016. Structural determinants of increased susceptibility to dehydration-induced cavitation in post-fire resprouting chaparral shrubs. *Plant Cell and Environment* **39**(11): 2473-2485.

Jansen S, Choat B, Pletsers A. 2009. Morphological Variation of Intervessel Pit Membranes and Implications to Xylem Function in Angiosperms. *American Journal of Botany* **96**(2): 409-419.

Jiang GF, Hinsinger DD, Strijk JS. 2016. Comparison of intraspecific, interspecific and intergeneric chloroplast diversity in Cycads. *Scientific Reports* **6**: 31473-31482.

Jiang GF, Li SY, Li YC, Roddy AB. 2022. Coordination of hydraulic thresholds across roots, stems, and leaves of two co-occurring mangrove species. *Plant physiology* **189**(4): 2159-2174.

Kaack L, Altaner CM, Carmesin C, Diaz A, Holler M, Kranz C, Neusser G, Odstrcil M, Schenk HJ, Schmidt V, et al. 2019. Function and three-dimensional structure of intervessel pit membranes in angiosperms: a review. *IAWA Journal* **40**(4): 673-702.

Kaack L, Weber M, Isasa E, Karimi Z, Li S, Pereira L, Trabi CL, Zhang Y, Schenk HJ, Schuldt B, et al. 2021. Pore constrictions in intervessel pit membranes provide a mechanistic explanation for xylem embolism resistance in angiosperms. *New Phytologist* **230**(5): 1829-1843.

Kipp MA, Stüeken EE, Strömberg CAE, Brightly WH, Arbour VM, Erdei B, Hill RS, Johnson KR, Kvaček J, McElwain JC, et al. 2023. Nitrogen isotopes reveal independent origins of N2-fixing symbiosis in extant cycad lineages. *Nature Ecology & Evolution*.

Larter M, Pfautsch S, Domec JC, Trueba S, Nagalingum N, Delzon S. 2017. Aridity drove the evolution of extreme embolism resistance and the radiation of conifer genus Callitris. *New Phytologist* **215**(1): 97.

Lens F, Gleason SM, Bortolami G, Brodersen C, Delzon S, Jansen S. 2022. Functional xylem characteristics associated with drought-induced embolism in angiosperms. *New Phytologist* **n/a**(n/a).

Lens F, Gleason SM, Bortolami G, Brodersen C, Delzon S, Jansen S. 2023. Comparative anatomy vs mechanistic understanding: how to interpret the diameter-vulnerability link. *IAWA Journal* **44**(3-4): 368-380.

Lens F, Sperry JS, Christman MA, Choat B, Rabaey D, Jansen S. 2011. Testing hypotheses that link wood anatomy to cavitation resistance and hydraulic conductivity in the genus Acer. *New Phytologist* **190**(3): 709-723.

Levionnois S, Jansen S, Wandji RT, Beauchene J, Ziegler C, Coste S, Stahl C, Delzon S, Authier L, Heuret P. 2021. Linking drought-induced xylem embolism resistance to wood anatomical traits in Neotropical trees. *New Phytologist* **229**(3): 1453-1466.

Li S, Lens F, Espino S, Karimi Z, Klepsch M, Schenk HJ, Schmitt M, Schuldt B, Jansen S. 2016. Intervessel pit membrane thickness as a key determinant of embolism resistance in angiosperm xylem. *IAWA Journal* **37**(2): 152-171.

Mamay SH. 1969. Cycads: Fossil evidence of late paleozoic origin. *Science* **164**(3877): 295-296.

Marler T. 2023. Stem Carbohydrate Richness in Two Cycad Species. *HortScience* **58**: 808-809.

McDowell N, Pockman WT, Allen CD, Breshears DD, Cobb N, Kolb T, Plaut J, Sperry J, West A, Williams DG. 2008. Mechanisms of plant survival and mortality during drought: why do some plants survive while others succumb to drought? *New Phytologist* **178**(4): 719-739.

Meng Y-Y, Xiang W, Wen Y, Huang D-L, Cao K-F, Zhu S-D. 2021. Correlations between leaf economics, mechanical resistance and drought tolerance across 41 cycad species. *Ann Bot*.

Miranda MT, Pereira L, Pires GS, Guan X, Silva LM, Kreinert S, Machado EC, Jansen S, Ribeiro RV. 2023. Xylem sap residue in cut-open conduits can affect gas discharge in pneumatic experiments. *bioRxiv*: 2023.2008.2008.552466.

Nadal M, Clemente-Moreno MJ, Perera-Castro AV, Roig-Oliver M, Onoda Y, Gulías J, Flexas J. 2023. Incorporating pressure–volume traits into the leaf economics spectrum. *Ecology letters* **26**(4): 549-562.

Nagalingum N, Marshall C, Quental T, Rai H, Little D, Mathews S. 2011. Recent synchronous radiation of a living fossil. *Science* **334**(6057): 796-799.

Norstog KJ, Nicholls TJ. 1997. *Biology of the cycads*. Ithaca, New York: Cornell University Press.

Olson ME, Pace MR, Anfodillo T. 2023. The vulnerability to drought-induced embolism-conduit diameter link: breaching the anatomy-physiology divide. *IAWA Journal* **44**(3-4): 335-354.

Orme D, Freckleton R, Thomas G, Petzoldt T, Fritz S, Isaac N, Pearse W. 2012. caper: Comparative Analyses of Phylogenetics and Evolution in R.

Pang YK, Qin LL, Zhang TH, Lei JY, Zhang Y, Roddy AB, Jiang GF. 2023. Coordination of intertracheid pit traits and climate effects among cycads. *Physiol Plant* **175**(3): e13924.

Pammenter NW, Vander Willigen C. 1998. A mathematical and statistical analysis of the curves illustrating vulnerability of xylem to cavitation. *Tree physiology* **18**(8-9): 589-593.

Paradis E, Schliep KP. 2018. ape 5.0: an environment for modern phylogenetics and evolutionary analyses in R. *Bioinformatics* **35 3**: 526-528.

Pereira L, Bittencourt PRL, Oliveira RS, Junior MBM, Barros FV, Ribeiro RV, Mazzafera P. 2016. Plant pneumatics: stem air flow is related to embolism – new perspectives on methods in plant hydraulics. *New Phytologist* **211**(1): 357-370.

Pereira L, Bittencourt PRL, Pacheco VS, Miranda MT, Zhang Y, Oliveira RS, Groenendijk P, Machado EC, Tyree MT, Jansen S, et al. 2020. The Pneumatron: An automated pneumatic apparatus for estimating xylem vulnerability to embolism at high temporal resolution. *Plant Cell and Environment* **43**(1): 131-142.

Pereira L, Kaack L, Guan X, Silva LM, Miranda MT, Pires GS, Ribeiro RV, Schenk HJ, Jansen S. 2023. Angiosperms follow a convex trade-off to optimize hydraulic safety and efficiency. *New Phytol*.

Pittermann J, Baer A, Sang Y. 2021. Primary tissues may affect estimates of cavitation resistance in ferns. *New Phytologist* **231**(1): 285-296.

Pittermann J, Choat B, Jansen S, Stuart SA, Lynn L, Dawson TE. 2010. The Relationships between Xylem Safety and Hydraulic Efficiency in the Cupressaceae: The Evolution of Pit Membrane Form and Function. *Plant physiology* **153**(4): 1919-1931.

Pittermann J, Limm E, Rico C, Christman MA. 2011. Structure–function constraints of tracheid-based xylem: a comparison of conifers and ferns. *New Phytologist* **192**(2): 449-461.

Pittermann J, Sperry JS, Hacke UG, Wheeler JK, Sikkema EH. 2005. Torus-Margo pits help conifers compete with angiosperms. *Science* **310**(5756): 1924-1924.

Pittermann J, Sperry JS, Wheeler JK, Hacke UG, Sikkema EH. 2006. Mechanical reinforcement of tracheids compromises the hydraulic efficiency of conifer xylem. *Plant Cell and Environment* **29**(8): 1618-1628.

Pittermann J, Stuart S, Dawson T, Moreau A. 2012. Cenozoic climate change shaped the evolutionary ecophysiology of the Cupressaceae conifers. *Proc Natl Acad Sci U S A* **109**: 9647-9652.

Powers JS, Vargas-G G, Brodribb TJ, Schwartz NB, Perez-Aviles D, Smith-Martin CM, Becknell JM, Aureli F, Blanco R, Calderón-Morales E, et al. 2020. A catastrophic tropical drought kills hydraulically vulnerable tree species. *Global change biology* **26**: 3122-3133.

Pratt RB, Castro V, Jacobsen AL. 2023. The functional significance of tracheids co-occurring with vessels in xylem of Eudicots suggests a role in embolism tolerance. *IAWA Journal*.

Qin L, Pang Y, Zhang T, An Y, Jiang G-F. 2022. Contrasting hydraulic safety margins of three cycads. *Guihaia* **42**(9): 1602-1611.

Revell LJ. 2012. phytools: an R package for phylogenetic comparative biology (and other things). *Methods in Ecology and Evolution* **3**(2): 217-223.

Roddy AB, Guilliams CM, Fine PVA, Mambelli S, Dawson TE, Simonin KA. 2023. Flowers are leakier than leaves but cheaper to build. *New Phytol* **239**(6): 2076-2082.

Roddy AB, Jiang GF, Cao KF, Simonin KA, Brodersen CR. 2019. Hydraulic traits are more diverse in flowers than in leaves. *New Phytologist* **223**(1): 193-203.

Rueden CT, Schindelin J, Hiner MC, DeZonia BE, Walter AE, Arena ET, Eliceiri KW. 2017. ImageJ2: ImageJ for the next generation of scientific image data. *Bmc Bioinformatics* **18**(1): 529.

Sack L, Pasquet-Kok J. 2011. Leaf pressure-volume curve parameters. *PrometheusWiki website: http://prometheuswiki. publish. csiro. au/tikiindex. php*: accessed 1 May 2014.

Sahney S, Benton MJ, Falcon-Lang HJ. 2010. Rainforest collapse triggered Carboniferous tetrapod diversification in Euramerica. *Geology* **38**(12): 1079-1082.

Schneider EL, Carlquist S, Chemnick JG. 2007. Scanning electron microscope studies of cycad tracheids. *South African Journal of Botany* **73**(4): 512-517.

Scholander PF, Bradstreet ED, Hemmingsen EA, Hammel HT. 1965. Sap Pressure in Vascular Plants: Negative hydrostatic pressure can be measured in plants. *Science* **148**(3668): 339-346.

Scholz A, Rabaey D, Stein A, Cochard H, Smets E, Jansen S. 2013. The evolution and function of vessel and pit characters with respect to cavitation resistance across 10 Prunus species. *Tree physiology* **33**(7): 684-694.

Simonin KA, Roddy AB. 2018. Genome downsizing, physiological novelty, and the global dominance of flowering plants. *Plos Biology* **16**(1): e2003706.

Simpson P. 1975. Anatomy and morphology of the Joshua Tree (Yucca brevifolia): an arborescent monocotyledon.

Skelton RP, Anderegg LDL, Diaz J, Kling MM, Papper P, Lamarque LJ, Delzon S, Dawson TE, Ackerly DD. 2021. Evolutionary relationships between drought-related traits and climate shape large hydraulic safety margins in western North American oaks. *Proceedings of the National Academy of Sciences* **118**(10): e2008987118.

Smith-Martin CM, Muscarella R, Ankori-Karlinsky R, Delzon S, Farrar SL, Salva-Sauri M, Thompson J, Zimmerman JK, Uriarte M. 2022. Hurricanes increase tropical forest vulnerability to drought. *New Phytologist* **235**(3): 1005-1017.

Song Y, Poorter L, Horsting A, Delzon S, Sterck F. 2022. Pit and tracheid anatomy explain hydraulic safety but not hydraulic efficiency of 28 conifer species. *J Exp Bot* **73**(3): 1033-1048.

Sperry JS, Donnelly JR, Tyree MT. 1988. A method for measuring hydraulic conductivity and embolism in xylem. *Plant, cell & environment* **11**(1): 35-40.

Sperry JS, Hacke UG, Wheeler JK. 2005. Comparative analysis of end wall resistivity in xylem conduits. *Plant Cell and Environment* **28**(4): 456-465.

Stevenson DW, Norstog KJ, Molsen DV. 1996. Midribs of cycad pinnae. *Brittonia* **48**(1): 67-74.

Suissa JS, Friedman WE. 2021. From cells to stems: the effects of primary vascular construction on drought-induced embolism in fern rhizomes. *New Phytologist*.

Tardieu F, Simonneau T. 1998. Variability among species of stomatal control under fluctuating soil water status and evaporative demand: modelling isohydric and anisohydric behaviours. *J Exp Bot*(49): 419-432.

Tavares JV, Oliveira RS, Mencuccini M, Signori-Müller C, Pereira L, Diniz FC, Gilpin M, Marca Zevallos MJ, Salas Yupayccana CA, Acosta M, et al. 2023. Basin-wide variation in tree hydraulic safety margins predicts the carbon balance of Amazon forests. *Nature* **617**(7959): 111-117.

Tomlinson PB, Ricciardi A, Huggett BA. 2018. Cracking the omega code: hydraulic architecture of the cycad leaf axis. *Ann Bot* **121**(3): 483-488.

Trueba S, Delzon S, Isnard S, Lens F. 2019. Similar hydraulic efficiency and safety across vesselless angiosperms and vessel-bearing species with scalariform perforation plates. *J Exp Bot*.

Tyree M, Zimmermann M. 2013. *Xylem structure and the ascent of sap*. New York: Springer Science & Business Media.

Tyree MT, Sperry JS. 1989. Vulnerability of xylem cavitation and embolism. *Annual Review of Plant Physiology & Plant Molecular Biology* **40**(1): 19-38.

Volaire F, Lens F, Cochard H, Xu H, Chacon-Doria L, Bristiel P, Balachowski J, Rowe N, Violle C, Picon-Cochard C. 2018. Embolism and mechanical resistances play a key role in dehydration tolerance of a perennial grass *Dactylis glomerata* L. *Ann Bot* **122**(2): 325-336.

Wang Z, Huang H, Wang H, Peñuelas J, Sardans J, Niinemets Ü, Niklas KJ, Li Y, Xie J, Wright IJ. 2022. Leaf water content contributes to global leaf trait relationships. *Nature communications* **13**(1): 5525.

Warton DI, Duursma RA, Falster DS, Taskinen S. 2012. smatr 3 – an R package for estimation and inference about allometric lines. *Methods in Ecology and Evolution* **3**(2): 257-259.

Wheeler JK, Sperry JS, Hacke UG, Hoang N. 2005. Inter-vessel pitting and cavitation in woody *Rosaceae* and other vesselled plants: a basis for a safety versus efficiency trade-off in xylem transport. *Plant, cell & environment* **28**(6): 800-812.

Whitelock L 2003. The Cycads.In Landry G. *Brittonia*. Portland, OR, USA: Timber Press. 90-90.

Wright IJ, Reich PB, Westoby M, Ackerly DD, Baruch Z, Bongers F, Cavender-Bares J, Chapin T, Cornelissen JHC, Diemer M, et al. 2004. The worldwide leaf economics spectrum. *Nature* **428**(6985): 821-827.

Zhang YJ, Sack L, Cao K-F, Wei X-M, Li N. 2017. Speed versus endurance tradeoff in plants: Leaves with higher photosynthetic rates show stronger seasonal declines. *Scientific Reports* **7**: 42085.

Zhang YJ, Cao KF, Sack L, Li N, Wei XM, Goldstein G. 2015. Extending the generality of leaf economic design principles in the cycads, an ancient lineage. *New Phytologist* **206**(2): 817-829.

Supporting Information

Additional Supporting Information may be found online in the Supporting Information section at the end of the article.

Fig. S1. Percentage of air discharged as a function of xylem water potential for 20 cycad species (a-t).

Fig. S2. Hydraulic safety margins of HSM_{50} (Minimum seasonal water potential – P_{50}) and HSM_{88} (Minimum seasonal water potential – P_{50}) values of different plant lineages.

Fig. S3. Macerations from rachises of four exampled cycads of *Cycas segmentifida*, *Cycas sexsaminifera*, *Encephalartos concinnus*, *Cycas revoluta*.

Fig. S4. Tracheid diameter (D_t) and length (L_t) of different plant lineages.

Fig. S5. Relationships among embolism resistance traits (P_{12}, P_{50}, P_{88}) and interconduit pit traits.

Fig. S6. Relationships among embolism resistance traits (P_{12}, P_{50}, P_{88}, HSM_{50}) and vessel or tracheid pit traits.

Fig. S7. Relationships among embolism resistance traits (P_{12}, P_{50}, P_{88}, HSM_{50}) and tracheids pit aperture traits.

Fig. S8. Canonical Correlation Analysis (CCA) of dimension 1 and 2 for vessel traits and safety traits (P_{min}, P_{12}, P_{50}, P_{88}).

Fig. S9. Principal component analysis (PCA) of selected 22 traits.

Fig. S10. Relationships among tracheid/vessel diameter (D_t or D_v) and length (L_t or L_v) and pit traits.

Table S1 Differences of hydraulic traits between Cycadaceae and Zamiaceae.

Table S2 Detailed results of phylogenetically corrected generalized least squares (PGLS) regressions for pairwise tracheid trait.

891 **Table S3** Detailed results of phylogenetically corrected generalized least squares (PGLS)
892 regressions for pairwise vessel trait.

893 **Table S4** Differences of conduit and pit traits between Cycadaceae and Zamiaceae.

894 **Table S5** Differences in pinna traits between Cycadaceae and Zamiaceae.

895 **Table S6** Correlations among hydraulic safety traits and PC1 and PC2 scores from principal
896 component analysis (PCA) analysis of the 20 cycad species.

897

898

899

900

901

902 **Figure legends**

903 **Fig. 1.** Anatomical images of selected cycad species. Light microscopy images depict cross-
904 section of rachises (a) *Cycas sexsaminifera*; (b) *Encephalartos manikensis*. (c-g) Light
905 microscopy images of tracheids, (h-l) scanning electron micrographs of vascular bundles
906 showing tracheids and vessels, and (m-q) transmission electron micrographs of inter-
907 tracheid pits for (c,h,m) *Cycas sexseminifera*, (d,i,n) *Encephalartos gratus*, (e,j,o)
908 *Encephalartos laurentianus*, (f,k,p) *Encephalartos manikensis*, and (g,l,q) *Encephalartos*
909 *sclavoi*. Note that the colored boxes in (l) depict the areas of different cell types: yellow is
910 the entire area of interest, blue is the area of tracheids, and red is the area of vessels.

911

912 **Fig. 2.** Percentage of air discharged as a function of xylem water potential for 20 cycad
913 species (a-t). All curves were adjusted by excluding points measured above the turgor loss
914 point. Dashed red lines indicate the P_{50}. The dark blue solid line marks the sigmoidal fit.

915

916 **Fig. 3.** Embolism resistance (P_{50} and P_{88}) among different plant lineages. Medians ±
917 interquartile ranges are depicted by black points and error bars on top of individual species
918 values (colored points). (a) P_{50} values for angiosperms (n = 954), gymnosperms (n = 354),
919 Cycadaceae (n = 10), Zamiaceae (n = 10), and pteridophytes (n = 18). (b) P_{88} values for
920 angiosperms (n = 692), gymnosperms (n = 256), Cycadaceae (n = 10), Zamiaceae (n = 10),
921 and pteridophytes (n = 14). Except for cycads, data include stems, trunks, and leaves of

922 woody plants downloaded from xylem functional traits database
923 (https://xylemfunctionaltraits.org/), and the data for five of the pteridophytes were sourced
924 from Suissa and Friedman (2021).
925
926 **Fig. 4.** Relationships among embolism resistance (P_{12}, P_{50}, P_{88}) and tracheid or vessel traits:
927 (a-c) tracheid diameter (D_t, n = 20); (d-f) tracheid length (L_t, n = 19); (g-i) cell wall
928 reinforcement (*CWR*, n = 20); (j-l) vessel diameter (D_v, n = 20); (m-o) vessel element length
929 (L_v, n = 20). Points and error bars indicate mean ± SE (n = 3 – 6 individual plants).
930 Cycadaceae are shown in blue points, and Zamiaceae are shown in yellow points.
931
932 **Fig. 5.** Relationships among hydraulic safety traits (P_{12}, P_{50}, P_{88}, HSM_{50}, HSM_{88}) and (a-e)
933 vessel and (f-j) tracheid proportions. Points and error bars indicate mean ± SE (n = 3 – 6
934 individual plants). Cycadaceae are shown in blue points, and Zamiaceae are shown in
935 yellow points.
936
937 **Fig. 6.** Relationships among hydraulic safety traits (P_{12}, P_{50}, P_{88}, HSM_{50}, HSM_{88}) and vessel or
938 tracheid pit traits: (a-e) vessel pit membrane fraction (F_{pf}, n = 20); (f-j) vessel pit surface
939 area (A_{pit}, n = 20); (k-o) tracheid pit membrane fraction (F_{pf}, n = 20); (p-t) tracheid pit
940 surface area (A_{pit}, n = 20). Points and error bars indicate mean ± SE (n = 3 – 6 individual
941 plants). Cycadaceae are shown in blue points, and Zamiaceae are shown in yellow points.
942
943 **Fig. 7.** Relationships between turgor lost point (Ψ_{tlp}) and (a) P_{50}, (b) P_{88}, (c) minimum
944 seasonal water potential (P_{min}), and (d) P_{12}. Points and error bars indicate mean ± SE (n = 3 –
945 6 individual plants). Cycadaceae are shown in blue points, and Zamiaceae are shown in
946 yellow points.
947
948 **Fig. 8.** Pairwise trait correlation matrix from the Canonical Correlation Analysis (CCA) to
949 determine correlations between vulnerability traits (P_{min}, P_{12}, P_{50}, P_{88}), and vessel traits
950 (vessel proportion, vessel diameter and hydraulic weighted vessel diameter D_v, vessel
951 element length L_v, vessel pit membrane fraction F_{pf}, vessel pit membrane area A_{pit}, vessel pit
952 shape R_{pit}, vessel pit density D_p, and pit membrane thickness T_{pm}).
953
954

955

956

957

958

959

960

961

962

963

964

965

966 **Table 1. The 20 cycad species for this study.**

Family	Species	Code
Cycadaceae	*Cycas debaoensis* Y.C.Zhong & C.J.Chen	Cd
	Cycas diannanensis Z.T.Guan & G.D.Tao	Cdi
	Cycas elongata (Leandri) D.Yue Wang	Ce
	Cycas ferruginea F.N.Wei	Cf
	Cycas guizhouensis K.M.Lan & R.F.Zou	Cg
	Cycas hainanensis C.J.Chen	Ch
	Cycas revoluta Thunb.	Cr
	Cycas segmentifida D.Yue Wang & C.Y.Deng	Cs
	Cycas sexseminifera F.N.Wei	Cse
	Cycas szechuanensis W.C.Cheng & L.K.Fu	Csz
Zamiaceae	*Ceratozamia latifolia* Miq.	Cla
	Ceratozamia subroseophylla Mart.-Domínguez & Nic.-Mor.	Csu
	Encephalartos concinnus R.A.Dyer & I.Verd.	Eco
	Encephalartos gratus Prain	Eg
	Encephalartos laurentianus De Wild.	El
	Encephalartos manikensis (Gilliland) Gilliland	Em
	Encephalartos sclavoi De Luca, D.W.Stev. & A.Moretti	Es
	Encephalartos tegulaneus Melville	Et
	Macrozamia moorei F.Muell.	Mm
	Zamia furfuracea L.f.	Zf

967

968 **Table 2. Definition of all traits for the study.**

Symbol	Definition	Unit
Pit traits of rachis from scanning and transmission electron microscopy		

D_{pms}	Diameter of the outer pit membrane along the shortest axis	µm
D_{pml}	Diameter of the outer pit membrane along the longest axis	µm
D_{pas}	Diameter of the outer pit aperture along the shortest axis	µm
D_{pal}	Diameter of the outer pit aperture along the longest axis	µm
A_{pit}	Interconduit pit surface area or interconduit pit membrane surface area	μm^2
A_{pa}	Intertracheid pit aperture surface area	μm^2
F_{pf}	Pit membrane fraction=proportion of pit membrane area per conduit wall area	%
F_{pa}	Pit aperture fraction = pit aperture surface area/pit membrane surface area	%
F_p	Pit fraction = mean fraction of the tracheid area occupied by intertracheid pits=$A_pA_t^{-1} = F_cF_{pf}$	%
F_c	Contact fraction = fraction of the total tracheid wall perimeter in contact with another tracheid	-
A_p	Total intertracheid pit membrane surface area per tracheid area= F_pA_t	$mm^2\ mm^{-2}$
A_t	Average tracheid wall area = $\pi D_hL_t^*$	mm^2
R_{pit}	Pit shape = ratio of the longest axis of outer pit membrane to the shortest axis	-
R_{pa}	Pit aperture shape = ratio of the longest axis of outer pit aperture to the shortest axis	-
D_p	Pit density=number of interconduit pits per conduit wall area	$no.\mu m^{-2}$
T_{pm}	Pit membrane thickness	nm
D_{pc}	Depth of pit chamber from membrane surface to inner edge of pit aperture	nm
Vessel proportion	Vessel proportion = Vessel surface vertical section area/Area of interested	%
Tracheid proportion	Tracheid proportion = Vessel surface vertical section area/Area of interested	%
Vessel number	Number of vessels in the area of interested from vertical section	%
Tracheid number	Number of tracheids in the area of interested from vertical section	%
Anatomical and physiological traits of rachis from light microscopy		
D_v or D_t	Hydraulically-weighted vessel or tracheid diameter	µm
D_h	Hydraulically-weighted conduit diameter	µm
K_{th}	Theoretical hydraulic conductivity	$kg\ m^{-1}\ MPa^{-1}\ s^{-1}$
N	Number of conduit = total conduit number of a cross section for rachis	-
T_d	Conduit density = total conduit number of a cross section for rachis/area of a cross section for rachis	$no.mm^{-2}$
T_w	Double conduit wall thickness	µm
CWR	Conduit cell wall reinforcement, the thickness to span ratio of tracheid, $(t/b)^2$	-
L_t or L_V	Tracheid length or vessel element length	µm
Physiological and functional traits		
SWC	Saturated water content	$g\ g^{-1}$
Ψ_{tlp}	Turgor loss point	MPa
C_T	Absolute capacitance	$mol\ m^{-2}\ MPa^{-1}$
RWC_{tlp}	Relative water content at turgor loss point	%
LMA	Leaf mass per area	$g\ m^{-2}$
P_{12}, P_{50}, P_{88}	Xylem water potential at 12%/50%/88% percentage of air discharged to the maximum air discharged	MPa
P_{min}	Midday water potential (Minimum seasonal water potential)	MPa
HSM_{50}, HSM_{88}	Hydraulic safety margins = $P_{min} – P_{50}$ or $P_{min} – P_{88}$	MPa

Table 3. Statistical differences of hydraulic safety, tracheid diameter, and tracheid length among plant lineages.

	P_{12} (-MPa)	P_{50} (-MPa)	P_{88} (-MPa)	HSM_{50} (MPa)	HSM_{88} (MPa)	D_t (μm)	L_t (μm)
Angiosperms	1.44 ± 0.06bc	2.80 ± 0.06b	4.75 ± 0.11a	0.08 ± 0.08b	2.15 ± 0.12ab	54.83 ± 3.04a	-
Pteridophytes	0.92 ± 0.11c	1.68 ± 0.15c	2.59 ± 0.18b	0.59 ± 0.24b	0.84 ± 0.21b	37.22 ± 2.65ab	8432.86 ± 1737.96a
Non-cycad gymnosperms	3.25 ± 0.12a	4.83 ± 0.13a	6.17 ± 0.19a	2.00 ± 0.17a	3.02 ± 0.23a	15.98 ± 0.63c	1583.80 ± 117.11b
Cycads	1.95 ± 0.12b	2.26 ± 0.15bc	2.57 ± 0.21b	0.88 ± 0.10ab	1.20 ± 0.14b	32.72 ± 0.94bc	6637.85 ± 445.49a

Note: Different letters indicate significant differences between taxa. Data for angiosperms and non-cycad gymnosperms were downloaded from xylem functional traits database (https://xylemfunctionaltraits.org//), and the data for pteridophytes were sourced from Suissa and Friedman (2021) and Pittermann et al. (2011). $P < 0.05$, one-way ANOVA, values are means ± standard errors. Hydraulic safety traits (P_{12}, P_{50}, P_{88}, HSM_{50}, HSM_{88}), tracheid diameter (D_t), and tracheid length (L_t).

Table 4. Statistical differences of vessel and tracheid traits for the 20 cycads in this study.

Characters	Vessel	Tracheid	T	Sig
Proportions	10.92±0.97	35.39±1.93	-11.33	**0.000****
Vessel or tracheid diameter (D_v or D_t)	32.30±1.19	32.72±0.94	-0.276	0.784
Vessel or tracheid length (L_v or L_t)	2.00±0.02	3.60±0.19	-8.385	**0.000****

pit membrane fraction (F_{pf})	34.61±1.37	54.39±1.50	-9.746	**0.000****
D_{pml}	8.97±0.27	8.53±0.21	1.289	0.205
D_{pms}	6.68±0.29	7.35±0.19	-1.899	0.066
Pit membrane area A_{pit}	48.53±3.22	50.43±2.14	-0.491	0.627
Pit shape (R_{pit})	1.42±0.058	1.18±0.03	3.775	**0.001****
Pit density (D_p)	0.008±0.000	0.01±0.001	-5.831	**0.000****

Note: values indicate mean ± SE (n = 20). *: significant difference (P < 0.05), **: significant difference (P < 0.01) from student's *t*-tests. Diameter of the outer pit membrane along the longest axis (D_{pml}) and shortest axis (D_{pms}).

Table 5. Canonical correlation analysis of vessel traits and embolism resistance. *: significant correlation (*P* < 0.05).

Dimension	Canonical Correlation	Rao's F	df1	df2	P
1	0.962	2.93	36	27.97	**0.002***
2	0.915	2.06	24	23.80	**0.042***
3	0.854	1.37	14	18.00	0.261
4	0.370	0.26	6	10.00	0.942

Table 6. Standardized canonical coefficients of anatomical and vulnerability traits for Dimension 1, 2 and embolism resistance traits of Table5.

Anatomical traits	Dimension 1	Dimension 2
vessel element length	7.51	5.56
vessel diameter	14.31	-20.10
vessel proportion	-2.97	2.56
vessel pit shape (R_{pit})	-1.16	5.00
vessel pit membrane area (A_{pit})	2.93	6.97
pit membrane thickness (T_{pm})	2.28	0.59
vessel pit membrane fraction (F_{pf})	-3.20	6.74
vessel D_v	-23.49	11.19
Embolism resistance traits		
minimum seasonal water potential (P_{min})	4.87	-5.16
P_{12}	89.54	1.44
P_{50}	-245.87	3.78
P_{88}	153.81	4.64

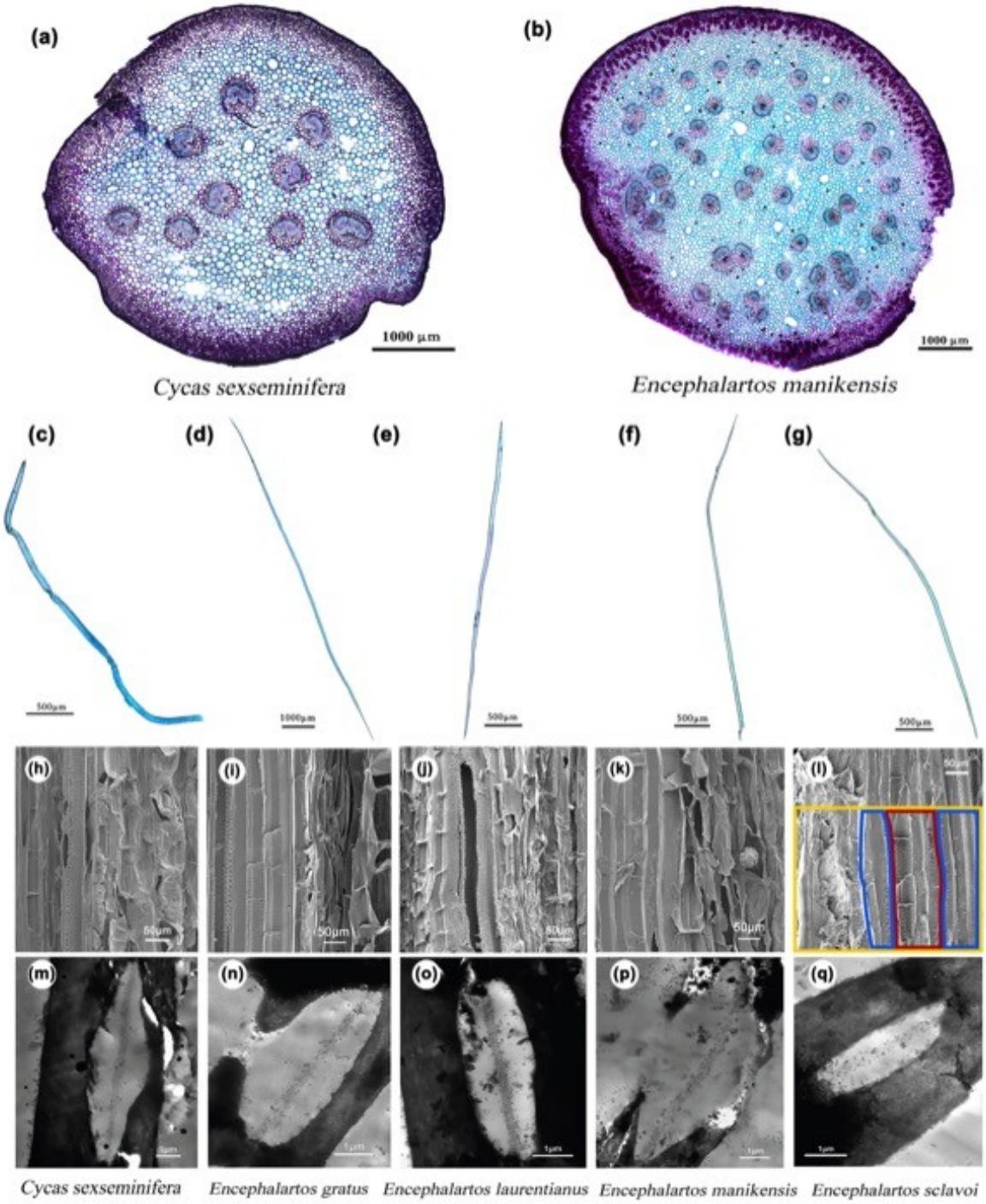
(a)
1000 µm
Cycas sexseminifera
(b)
1000 µm
Encephalartos manikensis
(c)
(d)
(e)
(f)
(g)
(h)
(i)
(j)
(k)
(l)
(m)
(n)
(o)
(p)
(q)
Cycas sexseminifera
Encephalartos gratus
Encephalartos laurentianus
Encephalartos manikensis
Encephalartos sclavoi

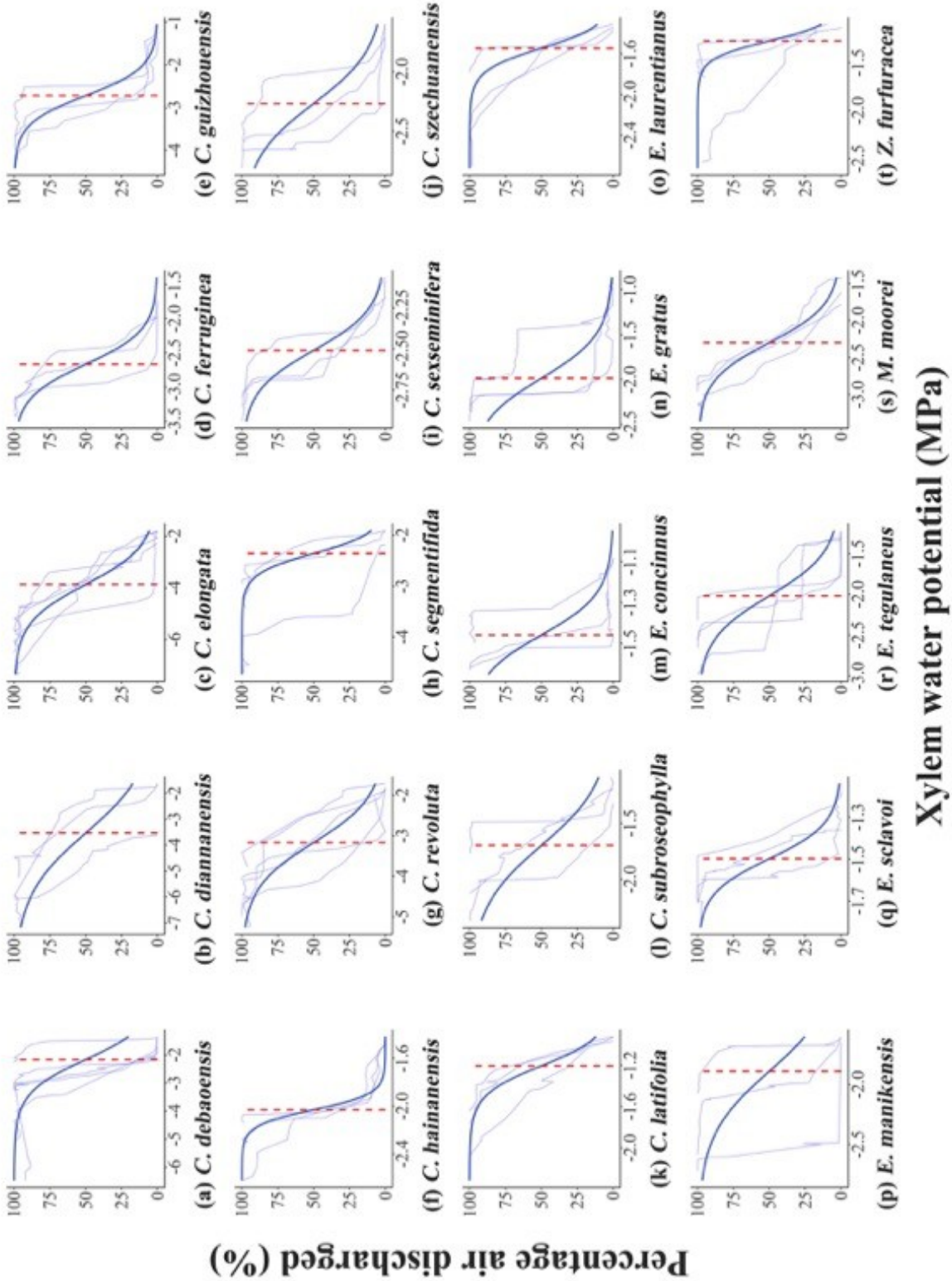
(a) C. debaoensis
(b) C. diannanensis
(c) C. elongata
(d) C. ferruginea
(e) C. guizhouensis
(f) C. hainanensis
(g) C. revoluta
(h) C. segmentifida
(i) C. sexseminifera
(j) C. szechuanensis
(k) C. latifolia
(l) C. subroseophylla
(m) E. concinnus
(n) E. gratus
(o) E. laurentianus
(p) E. manikensis
(q) E. sclavoi
(r) E. tegulaneus
(s) M. moorei
(t) Z. furfuracea
Percentage air discharged (%)
Xylem water potential (MPa)

1031

1032

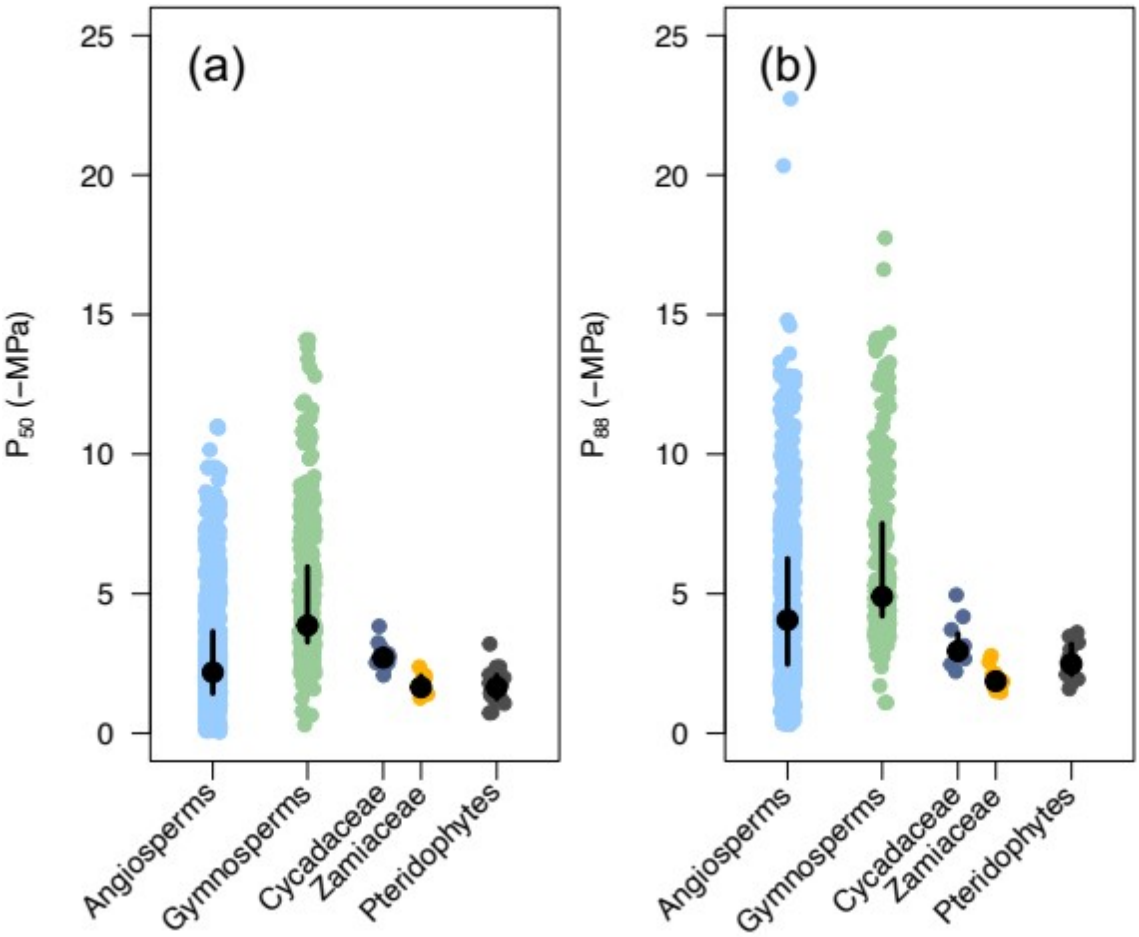
(a)
(b)
P_{50} (−MPa)
P_{88} (−MPa)
25
20
15
10
5
0
Angiosperms
Gymnosperms
Cycadaceae
Zamiaceae
Pteridophytes

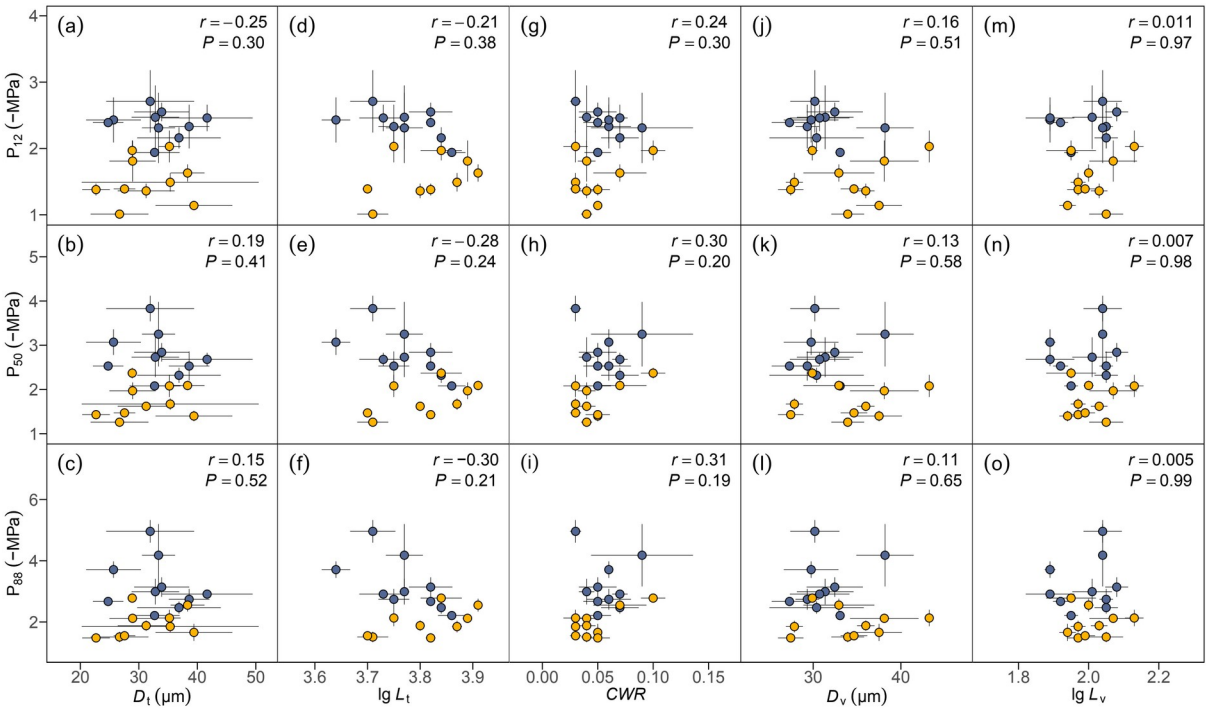
(a) r = −0.25 P = 0.30
(d) r = −0.21 P = 0.38
(g) r = 0.24 P = 0.30
(j) r = 0.16 P = 0.51
(m) r = 0.011 P = 0.97
(b) r = 0.19 P = 0.41
(e) r = −0.28 P = 0.24
(h) r = 0.30 P = 0.20
(k) r = 0.13 P = 0.58
(n) r = 0.007 P = 0.98
(c) r = 0.15 P = 0.52
(f) r = −0.30 P = 0.21
(i) r = 0.31 P = 0.19
(l) r = 0.11 P = 0.65
(o) r = 0.005 P = 0.99
P12 (−MPa)
P50 (−MPa)
P88 (−MPa)
Dt (μm)
lg Lt
CWR
Dv (μm)
lg Lv

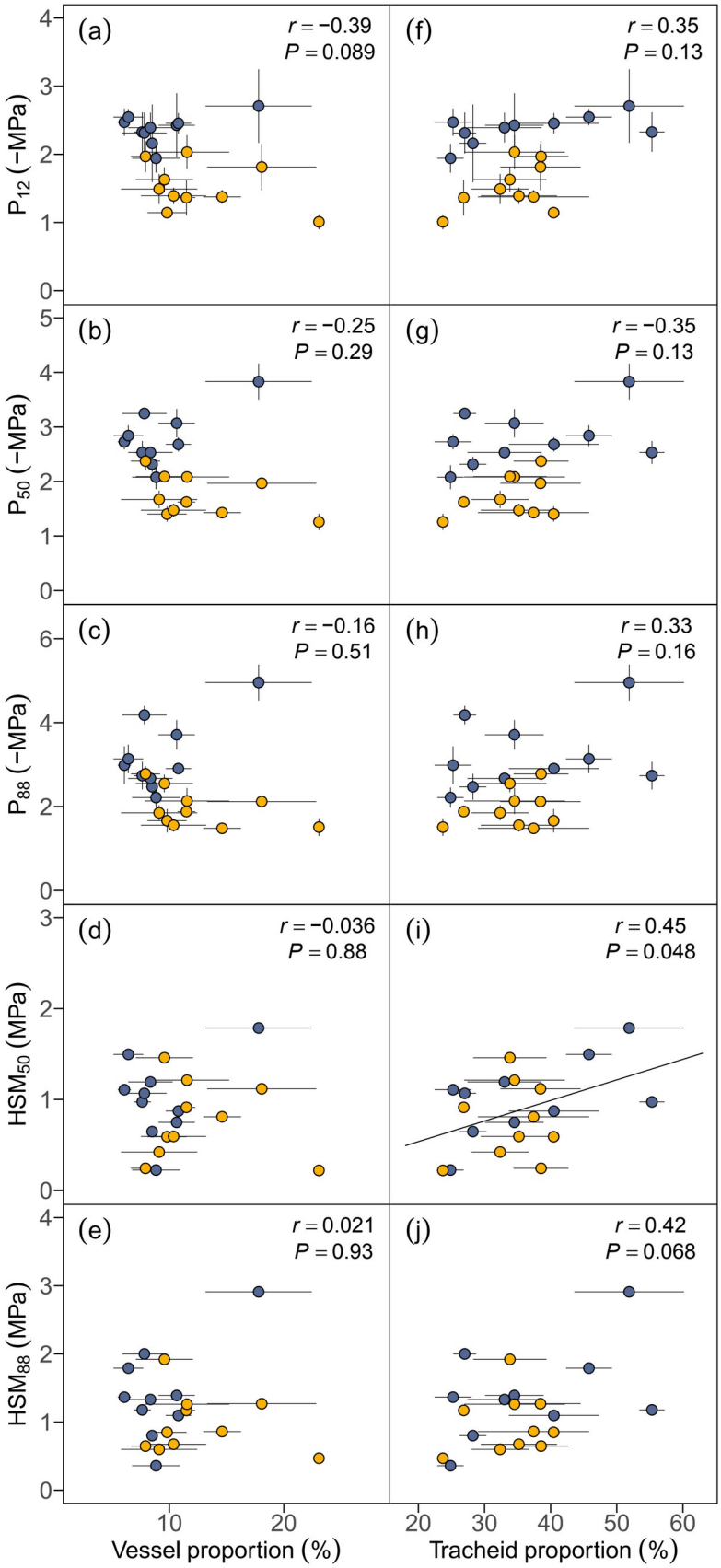
(a)
r = −0.39
P = 0.089
(f)
r = 0.35
P = 0.13
(b)
r = −0.25
P = 0.29
(g)
r = −0.35
P = 0.13
(c)
r = −0.16
P = 0.51
(h)
r = 0.33
P = 0.16
(d)
r = −0.036
P = 0.88
(i)
r = 0.45
P = 0.048
(e)
r = 0.021
P = 0.93
(j)
r = 0.42
P = 0.068
P12 (−MPa)
P50 (−MPa)
P88 (−MPa)
HSM50 (MPa)
HSM88 (MPa)
Vessel proportion (%)
Tracheid proportion (%)

1038

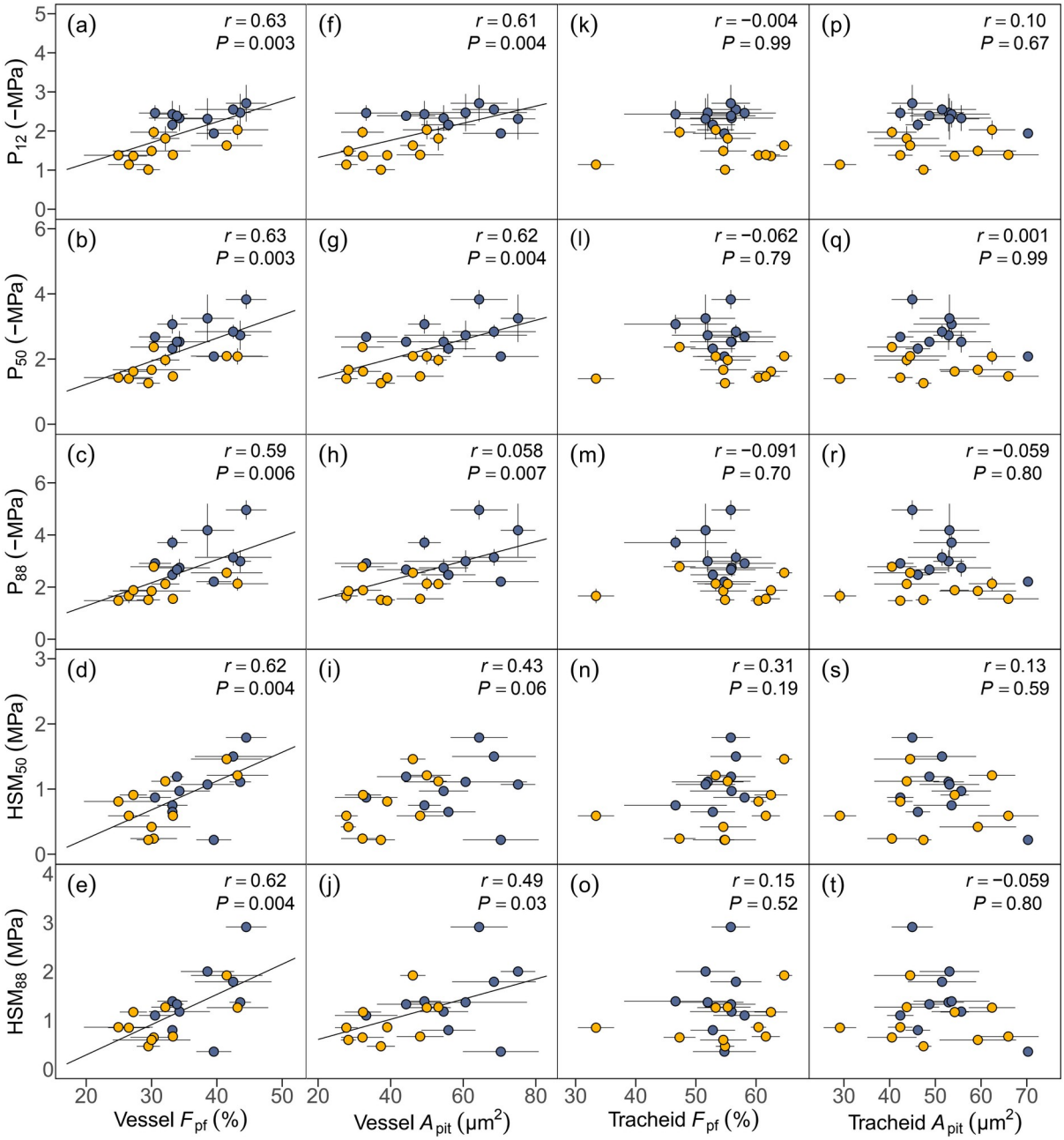
(a) r = 0.63 P = 0.003
(f) r = 0.61 P = 0.004
(k) r = −0.004 P = 0.99
(p) r = 0.10 P = 0.67
(b) r = 0.63 P = 0.003
(g) r = 0.62 P = 0.004
(l) r = −0.062 P = 0.79
(q) r = 0.001 P = 0.99
(c) r = 0.59 P = 0.006
(h) r = 0.058 P = 0.007
(m) r = −0.091 P = 0.70
(r) r = −0.059 P = 0.80
(d) r = 0.62 P = 0.004
(i) r = 0.43 P = 0.06
(n) r = 0.31 P = 0.19
(s) r = 0.13 P = 0.59
(e) r = 0.62 P = 0.004
(j) r = 0.49 P = 0.03
(o) r = 0.15 P = 0.52
(t) r = −0.059 P = 0.80
P12 (−MPa)
P50 (−MPa)
P88 (−MPa)
HSM50 (MPa)
HSM88 (MPa)
Vessel Fpf (%)
Vessel Apit (μm2)
Tracheid Fpf (%)
Tracheid Apit (μm2)

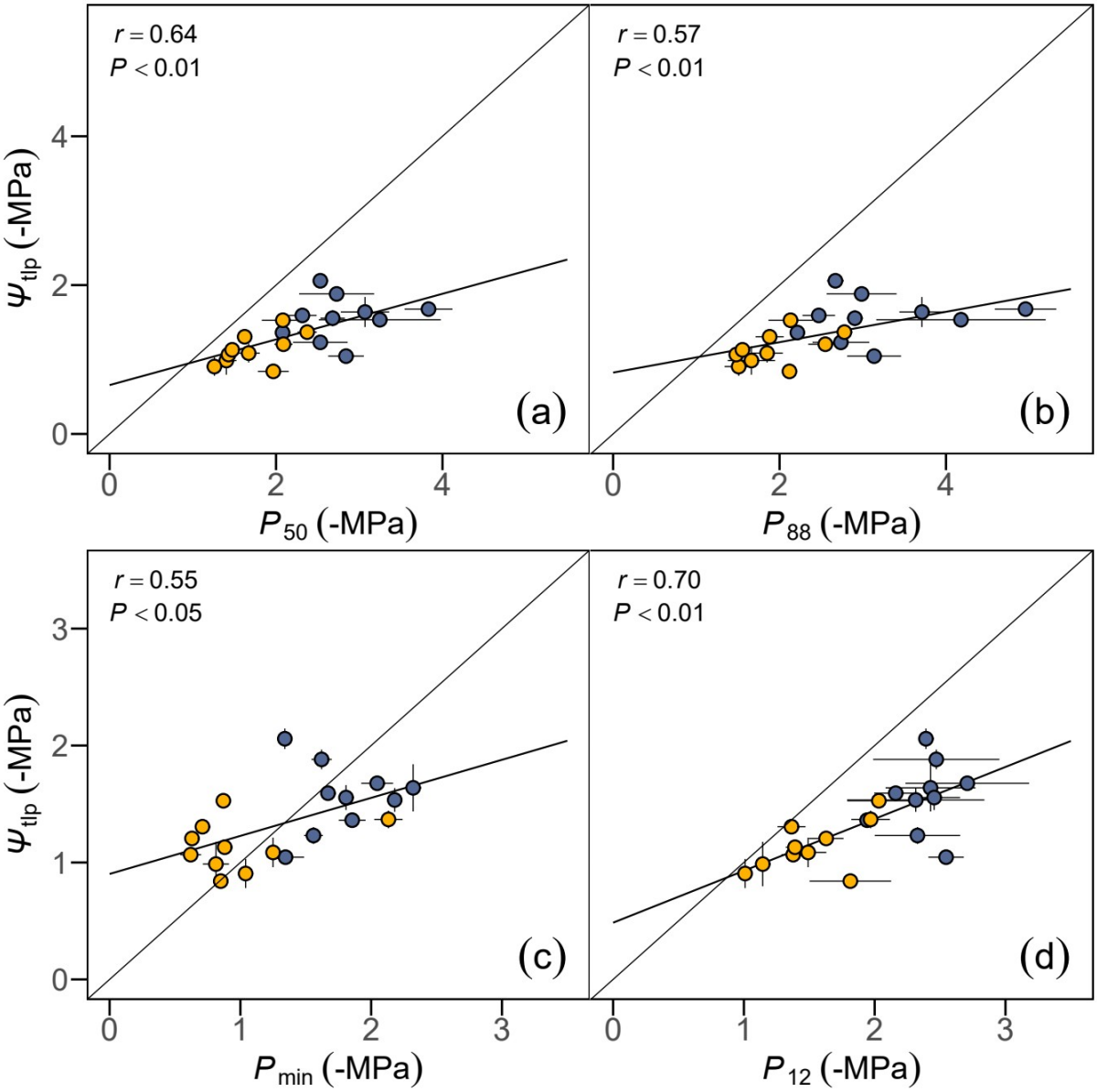
r = 0.64
P < 0.01
(a)
r = 0.57
P < 0.01
(b)
r = 0.55
P < 0.05
(c)
r = 0.70
P < 0.01
(d)
Ψtlp (-MPa)
P50 (-MPa)
P88 (-MPa)
Pmin (-MPa)
P12 (-MPa)

1042

1043

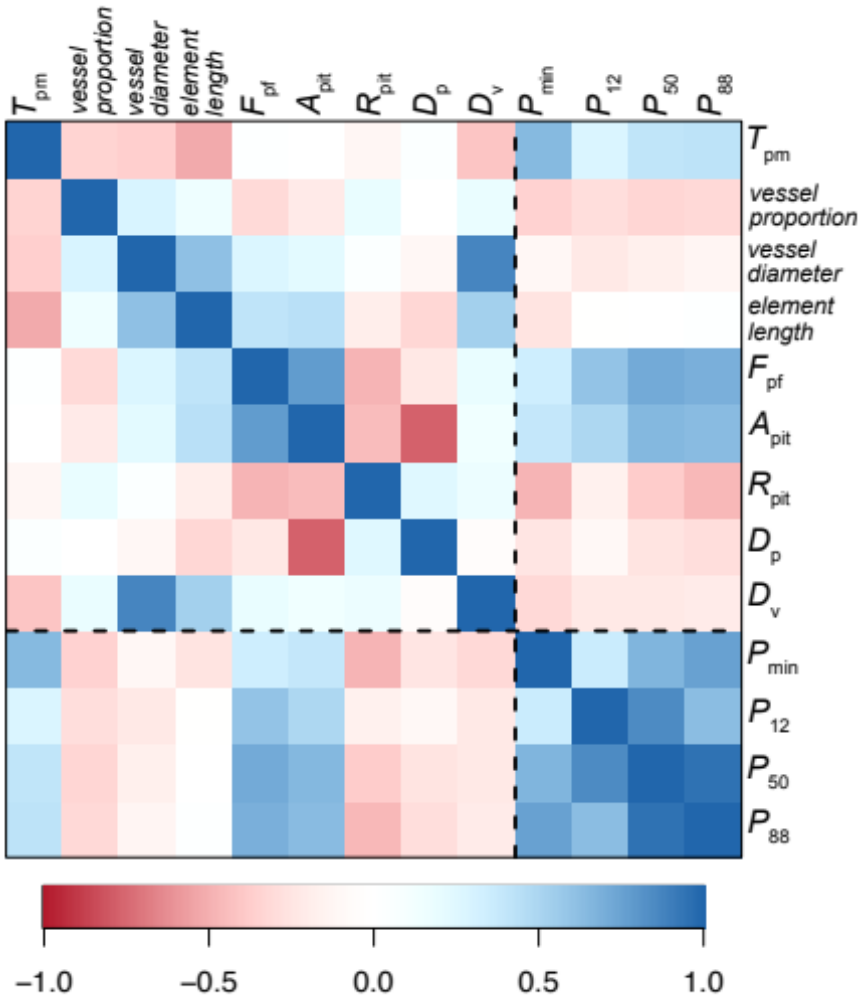
T_{pm}
vessel proportion
vessel diameter
element length
F_{pf}
A_{pit}
R_{pit}
D_p
D_v
P_{min}
P_{12}
P_{50}
P_{88}
−1.0
−0.5
0.0
0.5
1.0

1044